I - A - 390

UNIVERSITY OF SOUTHAMPTON

institute of sound and vibration research

THE DYNAMIC IN-PLANE RESPONSE AT THE CENTRE OF A ROTATING ELASTIC DISC DUE TO OSCILLATORY IN-PLANE FORCES AT THE RIM

R. J. Pinnington

ISVR Technical Report No. 121

October 1982

THE DYNAMIC IN PLANE RESPONSE AT THE CENTRE OF A ROTATING ELASTIC DISC DUE TO OSCILLATORY IN PLANE FORCES AT THE RIM

ISVR Technical Report 121

by

R.J. Pinnington

October 1982

Author. R.J. Pinnington
R J Pinnington

Group Chairman. R.G. White
R G White

ACKNOWLEDGEMENTS

The author gratefully acknowledges the support by the Ministry of Defence (Admiralty Marine Technology Establishement) of the unclassified contract under which this research was carried out.

CONTENTS

NOMENCLATURE

α force oscillation frequency in radians/sec

β phase of the transfer function $W(w)$

ϕ the inclination of a force at the rim to the normal

Ω force rotational frequency in rads/sec

η loss factor

ρ density

$\sigma_o(\theta,t), \tau_o(\theta,t)$ normal and shear stress distributions in the boundary, (time domain)

$\sigma_o(\theta,w)$. $\tau_o(\theta,w)$ Fourier transform of normal and shear stress distribution in the boundary

$\bar{\sigma}_{oc}, \bar{\sigma}_{os}, \bar{\tau}_{oc}, \bar{\tau}_{os}$ modal, normal and shear stress

$\bar{\sigma}_o = \bar{\sigma}_{oc} + i\bar{\sigma}_{os}, \bar{\tau}_o = \bar{\tau}_{oc} + i\bar{\tau}_{os}$

μ, λ Lamé constants, equation A1.3

ν Poissons ratio

ω angular frequency ($2\pi f$)

$\bar{\psi}$ the Fourier Transform of the angular acceleration at the centre of the disc

a_x, a_y the accelerations in the x,y directions at the centre of the disc

a radius of disc

A_{jn}, B_{jn} amplitudes of the n^{th} dilatational and rotational modes, $j=1,2$

c_1, c_2 dilatational and rotational wave speeds

E Youngs Modulus

f frequency

$\bar{H}(\omega)$ transfer inertance between a normal force applied to the rim and the acceleration at the centre in the same direction

i $\sqrt{-1}$

I moment of inertia

$J_n(z)$, $J_n'(z)$ Bessel function of the first kind of order n, and first derivative

k_1 dilatational wavenumber

k_2 rotational wavenumber

k_p longitudinal wave plate wavenumber

m	disc mass
n	circumferential mode number
P,Q	normal and shear force applied to the disc rim
r,θ	plane polar co-ordinates
t	time in secs
$\overline{T}(\omega)$	transfer inertance between a net moment applied to the rim angular acceleration of the centre of the disc
u,v	displacements in the x and y directions
$\overline{u},\overline{v}$	Fourier transform of the displacements in the x and y directions
$\overline{u}(r),\overline{v}(r)$	Fourier transform of the displacements in the x and y directions on the θ=0 radius
$\overline{U}_{jn},\overline{V}_{jn}$	Fourier transform of x and y displacements, for the n=1, for θ = 0, j=1,2.
$\overline{W}(\omega)$	Transfer inertance between a tangential force on the rim to the acceleration in the same direction at the centre of the disc.

1.0 INTRODUCTION

The moving parts of a rotating machine, are usually an assemblage of discs, as in a gearbox, or a simple thick disc or cylinder, as in an electric machine. The rotating disc element is acted upon by in plane forces at the rim, which are responsible for vibration at the shaft at the centre of the disc. These vibrations are then transmitted through the bearings to the machine casing, where they will cause unwanted sound radiation or vibration transmission to further connected structures.

The objective of this report is to consider the first part of the problem, namely to analyse the vibration response at the centre of a rotating disc which is subjected to in-plane, normal and tangential forces at the rim.

Such a disc will, of course, behave as a rigid body at low frequencies, with the acceleration at the centre in phase with force at the rim. However, to analyse the response at higher frequencies it is necessary to consider wave motion within the disc.

The inplane vibration of an elastic solid media arises from independent contributions of two types of wave motion, namely dilatational waves (which are equivalent to acoustic pressure waves in a liquid), and rotational (or shear) waves [1,2]. The vibration analysis of the disc therefore involves two uncoupled wave equations (associated with each wave type), expressed in plane polar co-ordinates. The general solution to each of these equations is a summation of orthogonal modes. Each mode has a Bessel function variation of order n in the radial direction and a sin $n\theta$ or cos $n\theta$ variation with the circumferential direction (where n is an integer between 0 and ∞).

Several authors have worked in this field previously. In general they analyse a stationary disc subjected to a rotating forcing point, as opposed to a rotating disc and a stationary forcing point. This simplifies the problem by ignoring Coriolis forces. The same approach is adopted here.

Eringen |3| provides general expressions for the vibration of a thick disc or cylinder subject to dynamic forces. His approach is largely followed in this report and his results applied to the specific problem of a point oscillating force applied to the disc, with normal and shear components. In references |4,5,6| thin discs or thin annular rings are analysed and resonance frequencies computed. The dilatational waves in a thin disc travel more slowly than in a thick disc as there is less lateral constraint, therefore the resonance frequencies associated with dilational wave motions differ slightly from those of a thick disc. The rotational waves are the same for a thin or thick disc.

In this report the analysis applies equally to a thin or thick disc, but resonance frequencies and transfer functions are only computed for the thick disc case.

The approach adopted in this report was first to calculate the transfer functions between normal, or tangential, forces at the disc rim and the inplane acceleration at the centre of the disc. Next the Fourier Transform of the excitation due to an oscillatory rotating point force was calculated; and finally the excitation and the transfer functions were combined to predict the response.

The greatest simplfications that arose from the transfer function calculations was that only modes with a cosθ or sinθ circumferential variation actually contribute to the inplane acceleration of the centre of the disc. It was also found that a normal force acting in the disc rim predominantly exciting dilatational wave motion, while a tangential force mainly excites rotational wave motion.

2.0 TRANSFER INERTANCE BETWEEN THE RIM AND THE CENTRE OF THE DISC

A complete analysis of the vibration of a disc subject to inplane boundary forces is presented in Appendix A1 (which is largely a modified version of reference 3). The results from that Section were applied to obtain an expression, for transfer inertance to the centre of the disc (inertance = acceleration/force). Using a digital computer these expressions were applied to give numerical data which are displayed graphically.

The analysis assumes a thick disc, for which the dilatational wave speed is greater than for a thin disc (because of Poisson's ratio effects). However, the theoretical form of the results is similar for both the thin or thick disc, the only difference being the value of the dilational wave number.

2.1 The Theoretical Form of the Transfer Inertances

The figure below gives the sign convention for the analysis:

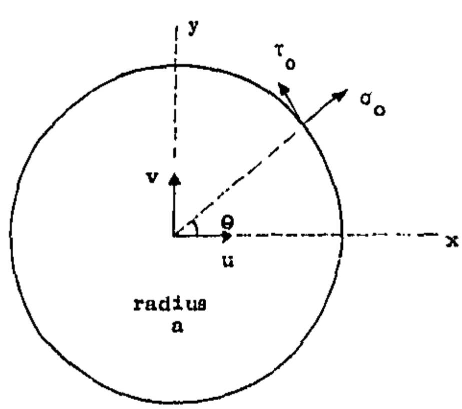

u and v are the displacements in the x and y directions. σ_o and τ_o are the surface stresses applied to the rim i.e. they act in the direction of the applied forces.

The displacements at any point on the x axis $\overline{u}(r)$, $\overline{v}(r)$ (in the x and y directions) are found by setting θ to zero in equation A1-15, giving

$$\overline{u}(r) = \sum_{n=0}^{\infty} \overline{U}_{2n}(r)$$

$$\overline{v}(r) = \sum_{n=0}^{\infty} \overline{V}_{n}(r) \qquad (2.1)$$

from which it can be seen that the displacement at any radius r, is the summation of modal contributions. $\overline{v}$ and $\overline{u}$ are the Fourier Transforms of the time dependent displacements v(t) defined as

$$\overline{v} = \int_{-\infty}^{\infty} v(t) e^{-i\omega t} dt \qquad (2.2)$$

where ω is the angular frequency and t the time.

The functions $\overline{U}_{2n}(r)$ and $\overline{V}_{n}(r)$ are the displacements made in the x and y directions at $\theta = 0$, for the n^{th} mode. These can be seen in equation A1.5 to be related to Bessel Functions of order n, (J_n).

The displacements in the x and y directions at the centre of the disc are simply found by substituting r=0 in equation 2.1 (coefficients in Equation A1.15) giving

$$\overline{v}(o) = -\frac{A_{11}}{2k_1} - \frac{B_{11}}{k_2} \qquad r = 0$$

$$\overline{u}(o) = -\frac{A_{21}}{2k_1} - \frac{B_{21}}{k_2} \qquad (2.3)$$

where k_1 and k_2 are the dilatational and rotational wave numbers respectively; and A_{11}, A_{21} are the amplitudes of the dilational n=1 mode and B_{11}, B_{21} are the amplitudes of the rotational n=1 mode. (Equation A1.14).

Only the n=1 dilational and rotational modes (which have a cos θ or sin θ circumferential variation and a J_1(kr) radial variation) contribute to the displacement at the centre of the disc. This is because the displacement is proportional to the gradient of the dilat ational mode shape and rotational mode shape, and only the n=1 Bessel function (J_1) has a slope at r=0. This is illustrated in the figures below.

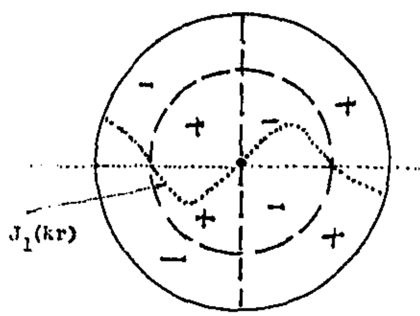

n=1 mode

The mode shape for (2,1) dilatational or rotational mode; 2 modal circles (including central point), 1 modal diameter

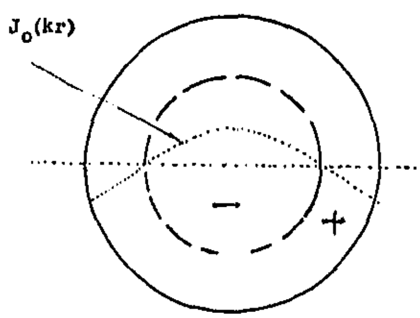

The approx. corresponding displacement mode shape adopts a (1,0) pattern with a finite value at the centre.

The displacements $\overline{u}(o)$ and $\overline{v}(o)$ at the centre of the disc can be written in terms of the applied forces at the rim by substituting for A_{11}, A_{21}, B_{11}, and B_{21} in equation 2.3 with the n=1 values of equaton A1.19, giving

$$-\omega^2\,\overline{v}(o) = \overline{H}(\omega).a\pi\overline{\sigma}_{os} + \overline{W}(\omega).\ a\pi\ \overline{\tau}_{oc} \tag{2.4}$$

$$-\omega^2\overline{u}(o) = \overline{H}(\omega).\ a\pi\ \overline{\sigma}_{oc} - \overline{W}(\omega).a\pi\ \overline{\tau}_{os}$$

where $$\overline{H}(\omega) = \frac{\omega^2}{2\mu D} \cdot \left[\frac{S_{21}(k_2a)}{2k_1} - \frac{S_{11}(k_1a)}{k_2} \right]$$

$$\overline{W}(\omega) = \frac{\omega^2}{2\mu D} \cdot \left[\frac{-N_{21}(k_2a)}{2k_1} + \frac{N_{11}(k_1a)}{k_2} \right]$$

$$D = N_{11}(k_1a).S_{21}(k_2a) - N_{21}(k_2a).S_{11}(k_1a)$$

$\overline{\sigma}_{oc}$, $\overline{\sigma}_{os}$ are related to the normal forces applied in the x and y directions and $\overline{\tau}_{oc}$ and $\overline{\tau}_{os}$ are related to the tangential forces applied in the y and x directions. These terms are defined in Equation A1-20 and discussed in Section 3.

On substituting for N_{11}, N_{21}, S_{11} and S_{21} from equation A1.17, the transfer inertances from the rim to the centre of the disc becomes, after some rearrangement,

$$\overline{H}(\omega) = \frac{1}{m} \cdot \frac{k_2a.\ J_2'(k_2a) - 2J_2(k_1a)}{\frac{2}{k_1a}.\ J_1(k_1a).k_2a\ J_2'(k_2a) - \frac{2J_1}{k_2a}(k_2a).2J_2(k_1a)} \tag{2.6}$$

$$\overline{W}(\omega) = \frac{1}{m}. \frac{-2J_2(k_2a) + k_1a(k_2/k_1)^2 J_1(k_1a) - 2J_2(k_1a)}{\frac{2}{k_1a}.J_1(k_1a).k_2aJ_2'(k_2a) - \frac{2J_1(k_2a)}{k_2a}.2J_2(k_1a)} \tag{2.7}$$

where $(\frac{k_2}{k_1})^2 = \frac{\lambda+2\mu}{\mu}$ and $m = \rho\pi a^2$ (2.?)

$\overline{H}(\omega)$ and $\overline{W}(\omega)$ are the transfer inertances between a point force on the rim and the acceleration response in the same direction at the centre of the disc, as defined in the figure below

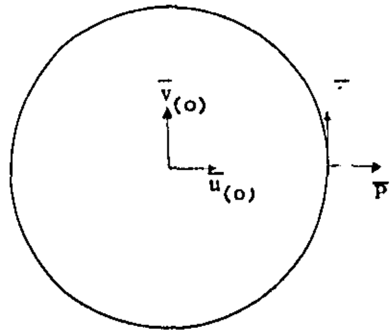

$$\overline{H}(\omega) = -\left.\frac{\omega^2\overline{u}(o)}{\overline{P}}\right|_{\overline{Q}=0} \qquad \left.\frac{\overline{v}(o)}{\overline{P}}\right|_{\overline{Q}=0} = 0 \qquad (2.9)$$

$$\overline{W}(\omega) = -\left.\frac{\omega^2\overline{v}(o)}{\overline{Q}}\right|_{\overline{P}=0} \qquad \left.\frac{\overline{u}(o)}{\overline{Q}}\right|_{\overline{P}=0} = 0$$

$\overline{P}_1$, $\overline{Q}$ are the Fourier Transforms of the applied forces to the rim

2.2 Computational Details

The transfer inertances $\overline{H}(\omega)$, $\overline{W}(\omega)$ and $\overline{T}(\omega)$ in equations 2.6, 2.7 and 2.8 were plotted out using a digital computer.

These functions are complex functions, with an imaginary component associated with the material damping.

The effect of the material damping was included by assuming that a complex modulus of elasticity $\overline{E} = E(1+i\eta)$, where η is the hysteretic loss factor. This complex modulus of elasticity is responsible for a complex wavenumber, $\overline{k}_2$ calculated thus (using A1.3)

$$\overline{k}_2 = k_2\left(1 - \frac{i\eta}{2}\right) = \omega\sqrt{\frac{2\rho(1+\nu)}{E(1+i\eta)}}$$

likewise

$$\overline{k}_1 = k_1(1 - \frac{i\eta}{2})$$

These values for complex wavenumbers were used as the argument of the Bessel Functions $J_1(\overline{k}a)$, $J_2(\overline{k}a)$ which control the transfer inertances. The complex Bessel functions J_1 and J_2 are shown in Figures 1 & 2.

The expressions used for the Bessel Functions in the computation are high and low frequency assymptopic solutions (see for example |8|).

The transfer functions were calculated for values $0 < k_2a < 20$ or $0 < k_2a < 100$. k_2a taken as the independent variable. 2048 data points were used to cover these frequency ranges.

The transfer functions were calculated for a range of k_1/k_2 ratios, including those for aluminium and steel.

2.3 Discussion of the Form of the Transfer Inertance H (ω)

The normal force transfer inertance, equation 2.6, is a function of several variables; the mass of the disc m, the rotational wavenumber k_2, the Poissons Ratio ν and the material loss factor, η. The significance of each of these variables is discussed in the following sections.

(i) The mass of the Disc

H(ω) normalised to the disc mass, is plotted for various Poisson's Ratio values in Figures 3-8. It can be seen that at low frequencies when $k_2a \leqslant 1$ the inertance taks the value of a rigid mass. For steel with a dilatational wave speed of 5700 m/s, $k_1/k_2 = .55$, a 2m diameter disc would behave as a rigid mass below 504 Hz.

(ii) The Poissons Ratio of the Material

Figures 3-6 show the transfer inertance for four different values of Poisson's ratio ν. The Poissons ratio is related to the ratio between the dilateral wavenumber (k_1) and rotational wavenumber k_2, for a thick disc by

$$k_1/k_2 = \sqrt{\frac{1-2\nu}{2-2\nu}} \qquad (2.10)$$

If the disc is thin the rotational wavenumber is unaffected but the dilatational wavenumber becomes that of a thin plate, longitudinal wave k_p and

$$\frac{k_p}{k_2} = \sqrt{\frac{1-\nu}{2}} \; . \qquad (2.11)$$

All the results in this analysis apply to thick discs but the thin disc results could be found using the ratio 2.11 in Equations 2.6 and 2.7.

Figure 3 displays the $\bar{H}(\omega)$, when only dilational waves are present in the disc, as would occur for a material so soft in shear as to be liquid. The dilatational waves correspond to acoustic pressure waves.

This function is obtained by setting $k_1/k_2 \rightarrow 0$ in equation 2.6, giving

$$H(\omega) = \frac{1}{m} . \frac{1}{2/(k_1 a) . J_1(k_1 a)} \qquad (2.12)$$

The resonances occur when $J_1(k_1 a) = 0$.

In Figure 3 the transfer inertance is displayed on a scale such that $k_1/k_2 = .55$ (the ratio for steel) which means that this graph displays the contribution to the transfer instance of a steel disc from the dilatational waves alone.

In Figures 4,5,6 the transfer inertance is plotted for Poisson's Ratios of 0, .28 and .33 respectively. A Poisson's ratio of .28 corresponds to steel and .33 to aluminium. Figure 5 shows $\bar{H}(\omega)$ for a steel disc (which has both dilatational and rotational wave transmission) obtained from equation 2.6 using $k_1/k_2 = .55$.

This plot is compared with the previously discussed case of dilatational wave transmission alone (Figure 3). It can be seen that the dilatational motion is responsible for the low frequency rigid body motion ($k_2a \leqslant 1$), and also for the overall trend.

However, indispersed between the dilatational wave resonances (denoted d) there is a train of approximately equally spaced resonances associated with rotational wave motion (denoted R). The steel is more mobile in rotational motion than dilatational motion (k_1/k_2 = .55) which is reflected by the fact that there are almost two rotational resonances to each dilatational resonance. Indeed the first significant resonance of the disc is mainly due to rotational motion and occurs when k_1a = 1.54 or k_2a = 2.79. For a 2m steel disc of dilational wave speed 5700 m/s this would correspond to a frequency of 1393 Hz.

In Section 2.4 it is shown that the rotational resonances occur when $J_2'(k_2a) = 0$, which for $k_2a > 4$, is approximately when $J_1(k_2a)=0$. The total transfer function $\overline{H}(\omega)$ can therefore be regarded as the superposition of two sets of resonant responses, one associated with dilatational motion, the other associated with rotational motion.

Figures 4 and 6 show $\overline{H}(\omega)$ for two different Poisson's ratios $\nu = 0$ and $\nu = .33$ respectively. It can be seen the k_2a value associated with rotational motion resonances are almost independent at Poisson's Ratio, as is clearly illustrated in Table 1 and Figure 7. This is of course because the values are plotted as a function of k_2a. The actual rotational wave resonance frequencies decrease with Poisson's ratio according to equation A1.5.

$$f = \frac{C_2}{2\pi}(k_2a) \qquad \text{where } C_2 = \sqrt{\frac{E}{2\rho(1+\nu)}} \qquad (2.13)$$

k_2 is constant

However, it is seen in Figures 4,6 and 7 that the dilational wave resonance frequencies increase relative to those associated with rotational motion, with increasing Poissons Ratio.

The resonance frequencies are given in Table 1 for various Poissons Ratios, although it must be stressed again that these refere to thick discs. For thin discs the resonance frequencies are tabulated in Table 2, which are taken from |4|.

The precise dilational or rotational mode shapes corresponding with resonance frequency in Table 1 have not been calculated, but the number of nodal circules (m) and nodal diameters (n) is indicated in Figure 7. All modes which contribute to the displacement of the centre have only one nodal diameter in the dilational or rotational mode shape as discussed in Section 2.1.

Figure 9 shows $\overline{H}(\omega)$ for a steel disc (ν = .33), loss factor .02, plotted for $0 < k_2 a < 100$, from which it can be seen that the damping heavily attenuates the contribution from the rotational waves leaving only the effect of the dilatational waves. Resonance frequencies occuring when $J_1(k_1 a) = 0$. Note that the modes are evenly excited, the centre of the disc always being an antinode for these modes.

2.4 The form of the transfer inertance $\overline{W}(\omega)$

$\overline{W}(\omega)$ the transfer inertance between a point tangential force at the rim of the disc and the acceleration response in the same direction at the centre of the disc is given in Equation 2.7. This equation is a function of the disc mass, the Poissons Ratio and the damping, is discussed in the following paragraphs.

(i) The Disc Mass

$\overline{W}(\omega)$ and $\overline{H}(\omega)$ are plotted together in Figure 15, a comparison reveals that at low frequencies where $k_2 a \leq 1$ they both take the same value of $\frac{1}{m}$, the inertance of a rigid mass.

(ii) The Effect of Poissons Ratio

The resonance frequencies of the $\overline{W}(\omega)$ function and the corresponding mode shapes are of course the same as those discussed previously for the $\overline{H}(\omega)$ function (Table 1, Figure 7). However, the degree of excitation of various modes is very different for the two functions. The $\overline{W}(\omega)$ function is dominated by the rotational wave motion, whereas the $H(\omega)$ function is dominated by the dilatational wave motion.

The dominance of the rotational wave motion over the dilatational wave motion is clearly seen in Figures 10-14. Figure 10 displays $\overline{W}(\omega)$ when the material is very soft in shear. For the computation it was chosen that

$$k_1/k_2 = 0.01$$

which is equivalent to $\nu \to .5$. For this case the rotational wave resonances displayed occur at much lower frequencies than the resonances associated with dilatational wave behaviour. Figure 10 is therefore the transfer inertance $\overline{W}(\omega)$ with no dilatational wave contribution.

However, inspection of Figures 11-14 reveals that for all values of Poissons Ratio $\overline{W}(\omega)$ is always dominated by the rotational wave motion, with behaviour closely resembling that of Figure 10.

A suitable approximation with which to describe the rotational wave motion contribution to $\overline{W}(\omega)$ is obtained by setting $k_1/k_2 = 0$. Under this condition Equation 2.7 becomes

$$\overline{W}(\omega) \simeq \frac{1}{m} \cdot \frac{2J_2(k_2a) - (k_2a)^2/2}{k_2a(J_2'(k_2a))} \qquad (2.14)$$

where

$$J_2'(k_2a) = J_1(k_2a) - \frac{2}{k_2a} J_2(k_2a).$$

This function is displayed in Figure 10. The rotational wave resonances occur when $J_2'(k_2a) = 0$. A further approximation can be made if $k_2a>>1$, then $\overline{W}(\omega)$ becomes

$$\overline{W}(\omega) \approx \frac{1}{m} \cdot \frac{}{\frac{2}{k_2a} J_1 (k_2a)} \qquad (2.15)$$

The equation is similar to the approximation for $\overline{H}(\omega)$ in Equation 2.12.

Figure 15 compares $\overline{H}(\omega)$ and $\overline{W}(\omega)$ for a steel disc with a loss factor of 0.02. The two functions assume their simplified forms (Equations 2.12 and 2.15) for $k_2a > 20$. It can be seen also that $\overline{W}(\omega)$ has almost twice as many resonances as $\overline{H}(\omega)$ and is usually at least twice as large as $\overline{H}(\omega)$. This reflects the fact that the vibration at the centre of a disc is usually at least twice as sensitive to tangential forces applied to the rim as compared to normal forces applied to the rim.

2.5 The form of the transfer inertance $\overline{T}(\omega)$

The rotation $\overline{\psi}$ at the centre of the disc can be deduced by setting r=0 in Equation A1.14. Only the n=0 modes have any contribution at r=0, as all Bessel Functions of the first kind, apart from J_o, are zero at the origin. The rotation of the centre therefore becomes

$$\overline{\psi} = B_{10} \qquad (2.16)$$

which on substitution for B_{10} from equation A1.9 gives

$$\overline{\psi} = \frac{1}{4u} \cdot \frac{}{S_{20}} \overline{\tau}_{oc} \qquad (2.17)$$

where τ_{oc} is proportional to the tangential force applied to the rim (see Equation 3.18). On substituting for S_{20} (from equation A1.17) and performing some manipulation.

$$-\omega^2 \, \overline{\psi} = \overline{T}(\omega) \, . \, \overline{\tau}_{oc} \; a^2 \pi \qquad (2.18)$$

$$\overline{T}(\omega) = \frac{1}{I} = \frac{1}{\left(\frac{8}{k_2 a}\right)^2 \cdot J_2(k_2 a)}$$

where $I = ma^2/2$, the moment of inertia area of the disc about the centre. $\overline{T}(\omega)$ is the transfer inertance between a unit moment applied to the disc rim, and the angular acceleration at the centre. At low frequencies $\overline{T}(\omega) = \frac{1}{I}$ as seen in Figure 16. The resonances of the n=0 modes occur when $J_2(k_2 a) = 0$, and therefore occur at different frequencies from the resonances in the $\overline{H}(\omega)$, $\overline{W}(\omega)$ transfer inertances.

These resonant frequencies are the same for a thin or a thick disc as there is no dilatational wave dependence.

In Figure 17 the transfer function $\overline{T}(\omega)$ is plotted $0 < k_2 a < 100$, the high frequency value becomes large compared to $\overline{H}(\omega)$ or $W(\omega)$ as it has a $(k_2 a)^2$ dependence (Equation 2.18) as compared to a $k_2 a$ dependence (Equation 2.6, 2.7).

3.0 THE EXCITATION FUNCTION

Section 2.1 was a derivation of the response of the centre of the disc in terms of: the point transfer functions $\overline{H}(\omega)$, $\overline{W}(\omega)$ and $\overline{T}(\omega)$ (between the centre and point forces on the disc rim), and the frequency dependent stress distributions $\bar{\sigma}_{oc}(\omega)$, $\bar{\sigma}_{os}(\omega)$ $\bar{\tau}_{oc}(\omega)$ and $\bar{\tau}_{os}(\omega)$ acting over the disc rim. The form of $\overline{H}(\omega)$, $\overline{W}(\omega)$ and $\overline{T}(\omega)$ was discussed in Sections 2.2 - 2.4 and it now remains to consider the form of the stress distributions $\bar{\sigma}_{oc}, \bar{\sigma}_{os}, \bar{\tau}_{oc}, \bar{\tau}_{os}$ in this section.

The analysis concentrates on the specific case of a point force oscillating at α rads/sec which rotates the disc at Ω rads/sec. However, the same procedures could be applied to more general stress distribution.

The stress functions $\bar{\sigma}_{oc}$, $\bar{\sigma}_{os}$, $\bar{\tau}_{oc}$ and $\bar{\tau}_{os}$ were found to be dependent upon the number of wavelengths 'n' in the circumferential disc mode shape, therefore as an introduction the simplest case of an oscillatory rotating force acting upon a rigid disc is considered first (as the motion is in phase over the whole body).

3.1 The Excitation Function of an Oscillatory Rotating Force acting upon a rigid disc

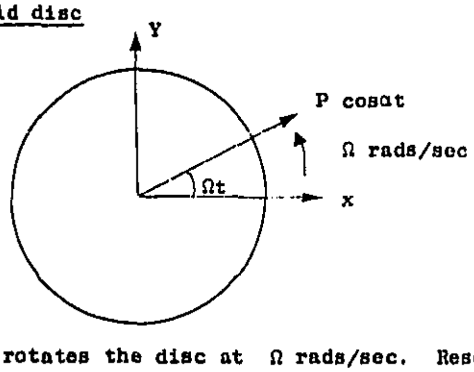

The force P cosαt rotates the disc at Ω rads/sec. Resolving the force into x and y coordinates gives

$$F_x = P\cos\alpha t.\cos\Omega t$$
$$F_y = P\cos\alpha t.\sin\Omega t \qquad (3.1)$$

These two forces can be combined using a vectorial notation by denoting a unit vector in the y direction as i, where $i = e^{\frac{i\pi}{2}}$, i.e.

$$\overline{F}(t) = F_x + iF_y = P\cos\alpha t . e^{i\Omega t} \tag{3.2}$$

Equation 3.2 is therefore a complete description of the magnitude and direction of the force at any time, the i term is not merely a mathematical device but has a physical meaning.

A Fourier Transform operation performed upon Equation 3.2, is defined

$$F(\omega) = \int_{-\infty}^{\infty} \overline{F}(t) e^{-i\omega t}\, dt \tag{3.3}$$

where $e^{-i\omega t}$ can be regarded as a vector rotating in a clockwise direction. On substitution of equation 3.2 into equation 3.3 and performing the integral by means of the identity

$$\int_{-\infty}^{\infty} e^{-i\omega t} dt = 2\pi\, \delta(\omega) \tag{3.4}$$

the Fourier Transform of the excitation becomes

$$\overline{F}(\omega) = P\pi \left| \delta(\omega-(\alpha+\Omega)) + \delta(\omega+(\alpha-\Omega)) \right| \tag{3.5}$$

which is purely real, hinting at its physical interpretation. Equation 3.5 displayed in graphical form is shown below

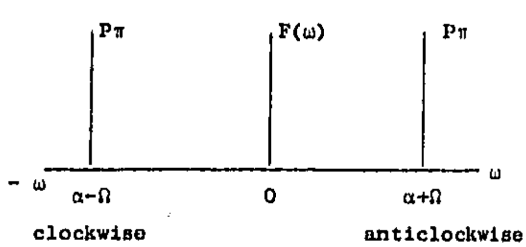

The Fourier Transform reveals that the excitation function in Equation 3.2 can be regarded as the superposition of two forces of constant magnitude, one spinning anti-clockwise (ω positive) with frequency $\alpha+\Omega$ rads/sec and the other spinning clockwise (ω negative) with frequency $\alpha-\Omega$ rads/sec.

Therefore this particular application of Fourier Transforms provides a physical interpretation to negative frequency.

The acceleration response of the disc is simply found by multiplying $\overline{F}(\omega)$ by the mass inertance $\frac{1}{m}$.

$$\overline{a}(\omega) = \frac{1}{m} \cdot \overline{F}(\omega) \tag{3.6}$$

By performing the inverse Fourier Transforms, given as

$$\overline{a}(t) = \frac{1}{2\pi} \int_{-\infty}^{\infty} a(\omega).e^{i\omega t}\, dt.$$

the acceleration in the time domain simply becomes

$$\overline{a}(t) = \frac{P}{m} \cdot \cos \alpha t.e^{i\Omega t} \tag{3.7}$$

as might be expected.

It must be noted that this approach is only possible when the disc is symmetrical and the transfer function $\frac{1}{m}$ is identical in the x and y directions, and the motions in the two directions are uncoupled.

3.2 The Excitation Functions for the disc modes with n circumferential wavelengths

In Section 3.1 only rigid body motion was considered, however it is the intention here to find the excitation level of disc modes which have n wavelengths around the circumference. For this analysis it is not sufficient to define the net force acting on the disc (i.e. P in Section 3.1) but the stress distribution over the surface must be stated.

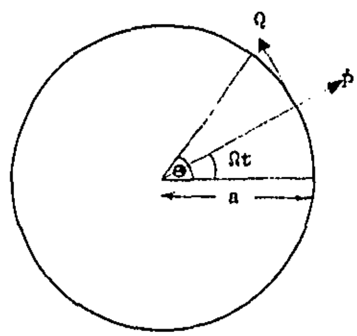

A general normal stress distribution $f(\theta)$ rotating the disc at Ω rads/sec and varying in magnitude at α rads/sec could be written as

$$\sigma_o(\theta,t) = f(\theta-\Omega t).\ \cos\alpha t$$

$$0 < \theta-\Omega t < 2\pi$$

However only a point force shall be considered here, although the same analysis could equally be applied to other stress distributions. Having said this, it will become clear later that if only the vibration of the centre of the disc is sought then only the net force is required, rather than the precise stress distribution.

Only normal forces will be considered in this analysis, but the derived expressions will be equally applicable to the shear forces.

For a point force $P\cos\alpha t$ acting normal to the disc rim, and rotating at Ω rads/sec, the stress distribution around the disc rim can be represented by

$$\sigma_o(\theta,t) = \frac{P}{a}\ .\cos\alpha t\ .\delta(\theta-\Omega t) \qquad (3.8)$$

$$0 < \theta-\Omega t < 2\pi$$

where $\delta(\theta-\Omega t)$ is repeated at 2π intervals of $(\theta-\Omega t)$. The periodically applied $\delta(\theta-\Omega t)$ function can be represented by a Fourier series, thus

$$\delta(\theta-\Omega t) = a_o + \sum_{n=1}^{\infty} a_n \cos n(\theta-\Omega t) + \sum_{n=1}^{\infty} b_n \sin n(\theta-\Omega t) \qquad (3.9)$$

where

$$a_o = \frac{1}{2\pi} \int_{-\pi}^{\pi} \delta(\theta-\Omega t) d(\theta-\Omega t) = \frac{1}{2\pi}$$

$$a_n = \frac{1}{\pi} \int_{-\pi}^{\pi} \delta(\theta-\Omega t) \cos n(\theta-\Omega t) . d(\theta-\Omega t) = \frac{1}{\pi}$$

$$b_n = \frac{1}{\pi} \int_{-\pi}^{\pi} \delta(\theta-\Omega t) \sin n(\theta-\Omega t) . d(\theta-\Omega t) . = 0$$

or

$$\delta(\theta-\Omega t) = \frac{1}{2\pi} + \frac{1}{\pi} \sum_{n=1}^{\infty} \cos n(\theta-\Omega t). \qquad (3.10)$$

Therefore the applied stress can be written as the product of cosine functions

$$\sigma_o(\theta,t) = \frac{p}{a\pi} .\cos\alpha t(\tfrac{1}{2} + \sum_{n=1}^{\infty} \cos n(\theta-\Omega t) \qquad (3.11)$$

which using the cosine addition rule becomes

$$\sigma_o(\theta,t) = \frac{p}{2a\pi} \left[\cos\alpha t + \tfrac{1}{2} \sum_{n=1}^{\infty} \cos((\alpha+n\Omega)t-n\theta)+\cos((\alpha-n\Omega)t+n\theta)\right] \qquad (3.12)$$

By inspection of the argument of the cosine terms it can be seen that for each mode number n, two cos $n\theta$ circumferential stress distributions occur simultaneously; one rotates anti-clockwise at $\alpha/n+\Omega$ rads/sec, and the other rotates clockwise at $\alpha/n-\Omega$ rads/sec. For n=0 the disc is subjected to a uniform pressure over the whole surface.

Equation 3.12 can be converted into the frequency domain by taking the Fourier Transforms defined in Equation 3.3, which (using identity 3.4) gives

$$\overline{\sigma}_o(\theta,\omega) = \frac{P}{2a}\{\delta(\omega-\alpha)+\delta(\omega+\alpha)$$

$$+\sum_{n=1}^{\infty} e^{in\theta}\left[\delta(\omega-\alpha+n\Omega)+\delta(\omega+\alpha+n\Omega)\right]$$

$$+\sum_{n=1}^{\infty} e^{-in\theta}\left[\delta(\omega+\alpha-n\Omega)+\delta(\omega-\alpha-n\Omega)\right]\} \tag{3.13}$$

This function is the boundary stress applied in the first of equations A1.16 and Equation A1-18, and it was shown that the particular stress functions $\overline{\sigma}_{oc}$ and $\overline{\sigma}_{oc}$ acting in the x and y directions can be found by applying equations A1.20, thus

$$\sigma_{oc} = \frac{1}{\pi}\int_o^{2\pi} \overline{\sigma}_o\ (\theta,\omega)\ \cos n\theta\ d\theta$$

$$\sigma_{os} = \frac{1}{\pi}\int_o^{2\pi} \overline{\sigma}_o\ (\theta,\omega)\ \sin n\theta\ d\theta\ . \tag{3.14}$$

A neater representation, is to use the i vector to indicate that the stress $\overline{\sigma}_{os}$ is in the vertical direction, and thus the stress functions can be combined vectorally as

$$\sigma_{oc} + i\sigma_{os} = \frac{1}{\pi}\int_o^{2\pi} \overline{\sigma}_o(\theta,\omega)\ e^{in\theta}\ d\theta\,. \tag{3.15}$$

By substituting for $\overline{\sigma}_o(\theta,\omega)$ (Equation 3.13) into 3.15 and performing the integration using equation 3.4, the stress function $\sigma_{oc}+i\sigma_{os}$ for the mode with n circumferential wavelengths becomes

$$\sigma_{oc}+i\sigma_{os} = \frac{P}{a}\left[\delta(\omega+\alpha-n\Omega)+\delta(\omega-\alpha-n\Omega)\right] \tag{3.16}$$

$$n=0 \rightarrow \infty$$

The interpretation of this is seen in the figure below

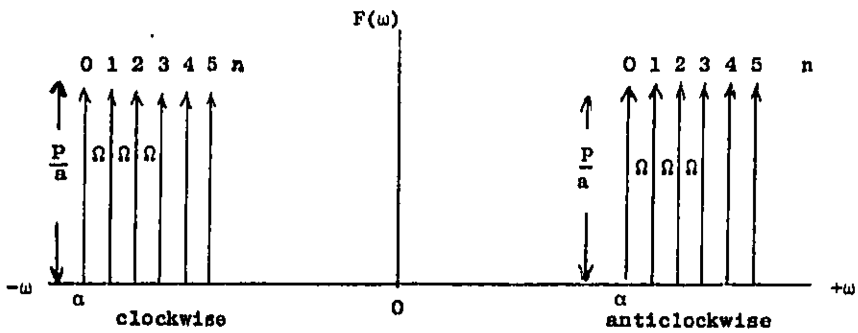

(i) It can be seen that each modes is excited equally by the stress of magnitude $\frac{P}{a}$.

(ii) At each excitation frequency α, and excitation rotation speed Ω and for each modenumber n, the disc is excited simultaneously by two stress distributions each with a spacial dependence of $\cos n\theta$. One stress distribution rotates anticlockwise at $\alpha/n+\Omega$ rads/sec and the other rotates clockwise at $\alpha/n-\Omega$ rads/sec, as shown below.

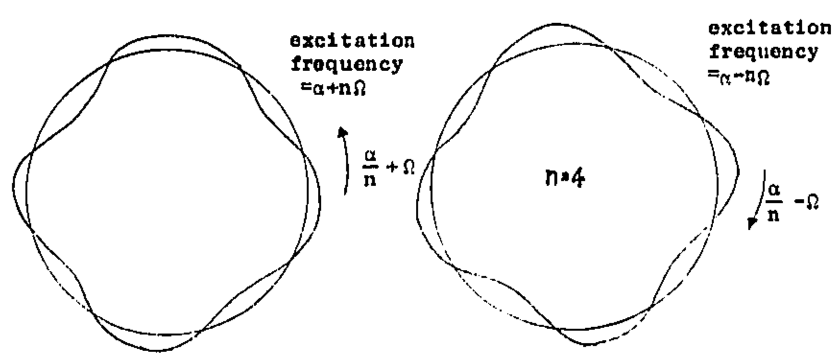

These two rotating modes are associated with, in a stationary plane of reference, two frequencies; $\alpha+n\Omega$ and $\alpha-n\Omega$ respectively.

(iii) When Ω is zero the two stress distributions associated wih the n^{th} mode rotates in opposite directions at the same frequency. The superposition of these two distribution results in a stationary or standing wave form, as is normally associated with vibration of static structures.

(iv) If the excitation frequency α is zero, i.e. a constant rotating force is applied, then the n^{th} mode is excited only in a anticlockwise direction at a speed of $n\Omega$ rads/sec with an associated frequency of $n\Omega$ rads/sec.

(v) For the analysis of the vibration at the centre of the disc only the n=1 mode contributes. The excitation function is

$$\sigma_o(\omega) = \sigma_{oc}+i\sigma_{os} = \frac{P}{a}\left[\delta(\omega+\alpha-\Omega) + \delta(\omega-\alpha-\Omega)\right] \qquad (3.17)$$

normal force loading. Likewise the shear force excitation is

$$\tau_o(\omega) = \tau_{oc}+i\tau_{os} = \frac{Q}{a}\left[\delta(\omega+\alpha-\Omega) + \delta(\omega-\alpha-\Omega)\right] \qquad (3.18)$$

where Q is the shear force applied at the same point as P.

The vibration at the centre of the disc is derived from the net force applied to the n=1 mode, which is the net force applied to the disc, as can be seen from Equation 3.14. Therefore the term P and Q in equations 3.17 and 3.18 refer generally to the net normal and shear force applied to the disc, irrespective of the load distribution.

4.0 THE ACCELERATION RESPONSE AT THE CENTRE OF THE DISC

In Equation 2.4 the Fourier Transform of the acceleration at the centre of the disc in the x and y directions is written as

$$a_y = -\omega^2 \overline{v} = \overline{H}(\omega).a\pi.\ \overline{\sigma}_{os} + \overline{W}(\omega).a\pi.\overline{\tau}_{oc} \qquad (4.1)$$

$$a_x = -\omega^2 \overline{u} = \overline{H}(\omega).a\pi.\ \overline{\sigma}_{oc} - \overline{W}(\omega).\ a\pi\ \overline{\tau}_{os}$$

However, because of the symmetry of the disc in the x and y directions the accelerations in the x and y directions can be combined vectorially thus

$$\overline{a}(\omega) = a_x + i\ a_y \qquad (4.2)$$

where i is $e^{i\frac{\pi}{2}}$, a unit vector in the y direction; $\overline{\sigma}_{oc}$, $\overline{\sigma}_{os}$, $\overline{\tau}_{oc}$ and $\overline{\tau}_{os}$ can likewise be defined in the manner of equation 3.17 and 3.18 as

$$\overline{\sigma}_o(\omega) = \overline{\sigma}_{oc} + i\ \overline{\sigma}_{os} \qquad (4.3)$$

$$\overline{\tau}_o(\omega) = \overline{\tau}_{oc} + i\overline{\tau}_{os}$$

then equation 4.1 can be expressed as

$$\underline{\overline{a}(\omega) = a\pi.\overline{H}(\omega).\overline{\sigma}_o + ia\pi\overline{W}(\omega).\overline{\tau}_o} \qquad (4.4)$$

The acceleration in the same instantaneous direction as the force given by $Re\{\overline{a}(\omega)\}$. While the acceleration leading the force by $\frac{\pi}{2}$ is given as

$$Im\ \{\overline{a}(\omega)\} \qquad (4.5)$$

The Fourier Transform of the acceleration vector $\overline{a}(\omega)$, resulting from the rotating oscillatory forces P(normal) and Q(shear), is found by substituting for $\overline{\sigma}_o$ and $\overline{\tau}_o$ (from equations 3.17 and 3.18) into equation 4.4 giving

$$a(\omega) = (\pi\ P.\overline{H}(\omega)+i\pi Q\overline{W}(\omega))(\delta(\omega+\alpha-\Omega)\ +\delta(\ \omega-\alpha-\Omega)). \tag{4.6}$$

The response in the time domain is found by taking the inverse Fourier transform of equation 4.6 i.e.

$$\overline{a}(t) = \frac{1}{2\pi}\int_{-\infty}^{\infty} \overline{a}(\omega)e^{i\omega t}\,d\omega \tag{4.7}$$

or

$$\overline{a}(t) = \tfrac{1}{2}\int_{-\infty}^{\infty} (P.\overline{H}(\omega)+iQ.\overline{W}(\omega).).(\delta(\omega+\alpha-\Omega)+\ (\omega-\alpha-\Omega))e^{i\omega t}\,d\omega \tag{4.8}$$

which on performing the integral gives

$$\begin{aligned} a(t) = {} & \tfrac{1}{2}\ (P\overline{H}(-\alpha+\Omega)+iQ\overline{W}(-\alpha+\Omega))e^{-i(\alpha-\Omega)t} \\ & +\tfrac{1}{2}\ (P\ \overline{H}(\alpha+\Omega)+iQ\overline{W}(\alpha+\Omega))e^{i(\alpha+\Omega)t} \end{aligned} \tag{4.9}$$

It is possible to procede further by making the following simplication. $\overline{H}(\omega)$ and $\overline{W}(\omega)$ are complex functions of (ω) having both a real and imaginary component. For physical structures the real component of the inertance is symmetrical about the ω= O point, while the imaginary component of inertance is assymetrical about $\omega=0$. Therefore the simple relationship exists that

$$\overline{H}^*(\omega) = \overline{H}(-\omega) \tag{4.10}$$

where * denotes the complex conjugate.

On making this substitution into Equation 4.9 the complex acceleration in the time domain, namely

$$\overline{a}(t) = a_x(t) + i\ a_y(t) \tag{4.11}$$

becomes

$$\boxed{\begin{aligned}\overline{a}(t) &= \tfrac{1}{2}\,(P.\overline{H}^*(\alpha-\Omega)+iQ\overline{W}^*(\alpha-\Omega))e^{-i(\alpha-\Omega)t} \\ &+\tfrac{1}{2}\,(P.\overline{H}(\alpha+\Omega) + iQ\overline{W}(\alpha+\Omega))e^{i(\alpha+\Omega)t}\end{aligned}} \quad (4.12)$$

If an inclined force $\overline{F}$ acting on the rim has normal and shear force components as shown below

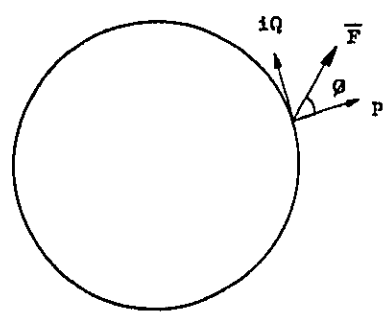

P and Q can be replaced by

$$\begin{aligned} P &= F\cos\phi \\ Q &= F\sin\phi \end{aligned} \quad (4.13)$$

4.1 Special Cases of the Response at the Centre of the Disc

The general expression for the response of the disc can be simplified for a few special cases:

(i) at low frequencies when $k_2a < 1$ the disc moves as a rigid body, and $\overline{H}(\omega)$, $\overline{H}^*(\omega)$, $\overline{W}(\omega)$ and $\overline{W}^*(\omega)$ are all equal to $\frac{1}{m}$, as in Figure 15 between points a and b. The response at the centre of the disc to a force inclined at ϕ radians from the normal is given from equations 4.12 and 4.13 as

$$\overline{a}(t) = \frac{F}{m}\, e^{i(\phi+\Omega t)} \cos\alpha t \quad (4.14)$$

where the applied force vector was

$$Fe^{i(\phi+\Omega t)}.\cos\alpha t \quad (4.15)$$

The response in the x and y directions are modulated cosine waves

$$a_x(t) = \frac{F}{m}\cos(\emptyset+\Omega t)\ \cos\alpha t$$
$$(4.16)$$
$$a_y(t) = \frac{F}{m}\sin(\emptyset+\Omega t)\ \cos\alpha t$$

as shown in the figure below

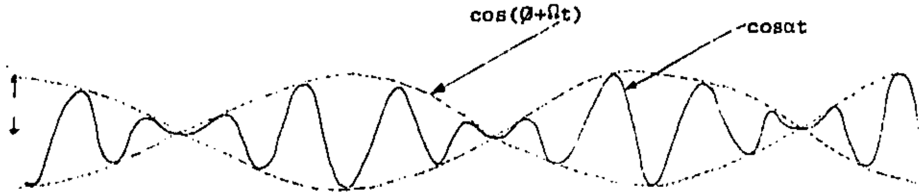

The acceleration tragectory on the x-y plane of an oscilloscope screen would be, for $\alpha=8\Omega$,

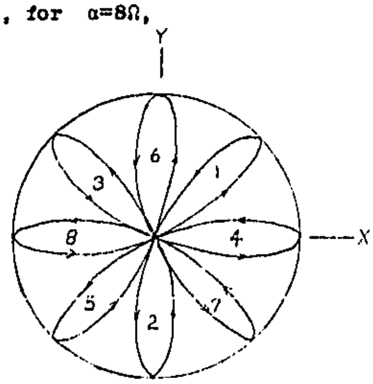

(ii) Between points b and c in Figure 15 it can be seen that the shearing force transfer inertance $\overline{W}(\omega)$ is much greater than the direct force transfer inertance. The transfer function $\overline{W}(\omega)$ changes only gradually with frequency, therefore $\overline{W}(\alpha+\Omega)\simeq\overline{W}(\alpha-\Omega)$ for $\alpha\gg\Omega$. Also for frequencies outside the resonant regions $\overline{W}(\omega)=\overline{W}^*(\omega) = |\overline{W}\ \ (\omega)|$. Therefore in this region the response takes the form

$$\overline{a}(t) \simeq F\sin\emptyset.|\overline{W}(\alpha)|.e^{i(\Omega t+\frac{\pi}{2})}\cos\alpha t \qquad (4.\ 17)$$

where the force vector was $F\ e^{i(\Omega t+\emptyset)}\cos\alpha t$

The response therefore leads the force by an angle of $\frac{\pi}{2} - \emptyset$.
For the alternative case when $\overline{H}(\omega) >> \overline{W}(\omega)$ the response would be

$$\overline{a}(t) = F \cos \emptyset . |\overline{H}(\omega)| . e^{i\Omega t} \cos\alpha t, \qquad (4.18)$$

indicating a lag of $\emptyset$ behind the force vector In both cases the responses would take the form of the previous two figures.

(iii) When the excitation frequency $\alpha+\Omega$ is equal, or very close to a resonance frequency of the disc (for example point d, Figure 15) only the terms containing $\alpha+\Omega$ in expression 4.12 are strongly excited. The acceleration response then takes the form

$$\overline{a}(t) \approx \frac{F}{2} (\cos\emptyset.\overline{H}(\alpha+\Omega) + i\sin\emptyset.\overline{W}(\alpha+\Omega))e^{i(\alpha+\Omega)t}$$

If it is now assumed that $\overline{H}(\alpha+\Omega)$ is neglected, on account of its relatively small size; the acceleration response can now be written as

$$\overline{a}(t) \approx \frac{F}{2} | \overline{W}(\alpha+\Omega) | e^{i(\beta+(\alpha+\Omega)t+\frac{\pi}{2})} \qquad (4.19)$$

where

$$| \overline{W}(\alpha+\Omega) | e^{i\beta} = \overline{W}(\alpha+\Omega)$$

This is a vector rotating in the anti-clockwise direction at $\alpha+\Omega$ radians/sec, i.e. the response, is due to the disc, in an n=1 mode shape spinning at $\alpha+\Omega$ rads/sec, as shown below

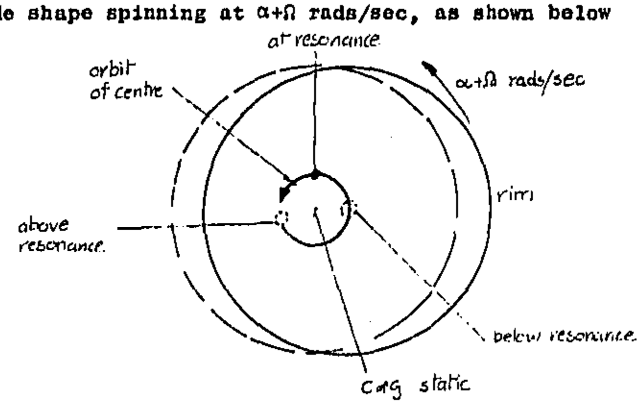

The precise phase depends strongly on β, which changes rapidly through the resonance region. The acceleration tragectory displayed in the x,y axis of an oscilloscope is a circle.

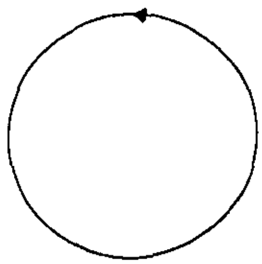

When the other excitation frequency $\alpha-\Omega$ coincides with the resonance frequency there is a similar result except that the acceleration vector rotates in the clockwise direction.

4.2 Response at the Centre of the Rotating Disc

All the previous analyses have been concerned with a stationary disc subject to a rotating force. However, the initial intention of the work was to solve the vibraton of a rotating disc subject to a stationary oscillating force. The general solution is easily found by multiplying equation 4.12 by $e^{-i\Omega t}$ which effectively applies a clockwise rotation to the disc. The solution becomes

$$\boxed{\begin{aligned}\overline{a}(t) &= \tfrac{1}{2}(P.\overline{H}^*(\alpha-\Omega)+iQ\overline{W}^*(\alpha-\Omega))e^{-i\alpha t}\\ &+\tfrac{1}{2}\,(P.\overline{H}(\alpha+\Omega)iQ\overline{W}(\alpha+\Omega))e^{i\alpha t}\end{aligned}} \qquad (4.20)$$

to a forcing function $Fe^{i\phi}\cos\alpha t$.

(i) In the mass controlled region the response is

$$\overline{x}(t) \simeq \frac{F}{m}e^{i\phi}.\cos\alpha t.$$

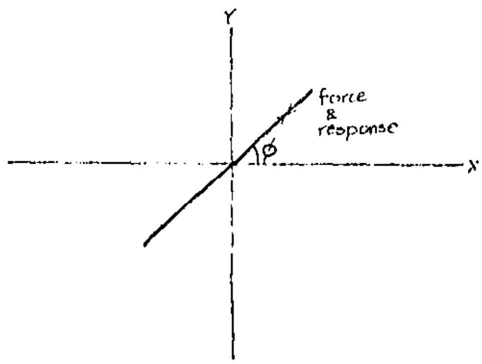

(ii) In the non-resonant region, (see Equation 4.18) the response is

$$\bar{a}(t) = \frac{F}{2}\sin\phi\,|\bar{W}(\omega)|.\; e^{i\frac{\pi}{2}}.\;\cos\alpha t \tag{4.21}$$

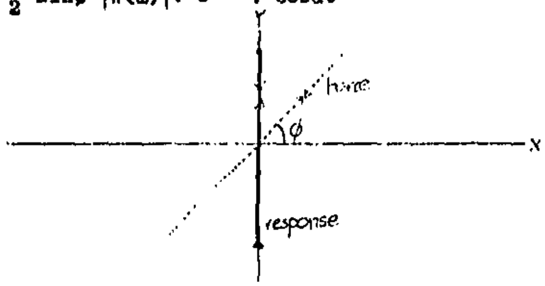

(iii) In the resonant region (see Equation 4.19) the response is

$$\bar{a}(t) = \frac{F}{2}|\,\bar{W}(\alpha+\Omega)|e^{i(\beta+\alpha t+\frac{\pi}{2})} \qquad (\alpha+\Omega\ =\ \text{resonance frequency, } \omega_n)$$

$$\text{or}\quad \bar{a}(t) = \frac{F}{2}\,|\bar{W}(\alpha-\Omega)|e^{i(-\beta-\alpha t\,+\frac{\pi}{2})} \qquad (\alpha-\Omega\ =\ \text{resonance frequency } \omega_n) \tag{4.22}$$

where $\bar{W}(\omega) = |W|e^{i\beta}$

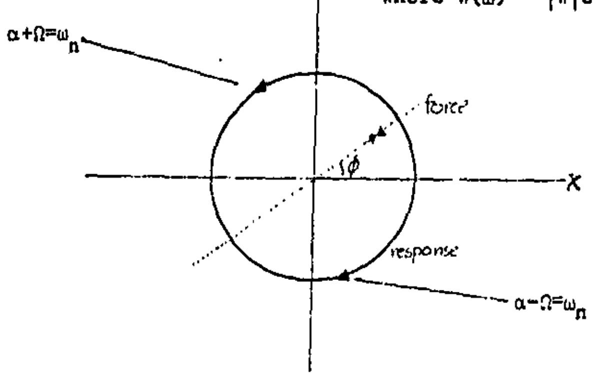

5.0 CONCLUSIONS

The results can be summarised into three sections, namely; the transfer functions, the excitation, the response at the centre of the disc due to the oscillating rotating force.

5.1 The Transfer Function

(i) The Transfer Function $\overline{H}(\omega)$ between a normal force and the acceleration response in the same direction, at the centre of the disc is largely governed by the dilatational wave motion. When $k_2a < 1$ the disc behaves as a rigid mass. Resonances associated with the dilatational wave motion occur approximately when $J_1(k_1a) = 0$.

(ii) The transfer function $\overline{W}(\omega)$ between a tangential force and the acceleration response in the same direction at the centre of the disc is dominated by the rotational wave transmission. This is responsible for the mass-like behaviour for $k_2a < 1$. Resonances associated with rotational wave motion occur approximately when $J_1(k_2a)=0$.

(iii) The $\overline{W}(\omega)$ and $\overline{H}(\omega)$ transfer functions are comprised only of Bessel Functions of order one (n=1) (which are associated with $\cos\theta$ or $\sin\theta$ circumferential mode shape).

(iv) The first resonance frequency arises from rotational wave motion, when $k_2a \approx 2.8$ (for steel).

(v) In general, vibration transmission to the centre of the disc is greater from a tangential force than from a normal force (i.e. ($\overline{W}(\omega)$ tends to be greater than $\overline{H}(\omega)$).

(vi) Angular acceleration at the centre of the disc is solely caused by n=0 rotational modes of vibration (those which have no variation in the θ direction). When $k_2a<1$ the angular acceleration is controlled only by the disc moment of inertia. Resonances occur approximately when $J_2(k_2a) = 0$.

5.2 The Excitation Function

(i) A point force which oscillates at frequency αrads/sec and rotates the disc in an anticlockwise direction of Ωrads/sec excites each mode at 2 different frequencies. A mode with n wavelengths in the circumferential direction is excited by an anticlockwise rotating stress distribution at $\Omega+\alpha/n$ rads/sec, and by a clockwise stress distribution at $\Omega-\alpha/n$ rads/sec. Each mode is excited at the same level by a point force.

(ii) The motion at the centre of the disc is only dependent upon the net force acting in the disc rim, and is independent of the load distribution.

5.3 The Response at the Centre of the Disc

(i) For a rotating disc and a stationary oscillating force the acceleration at the centre of the disc is necessarily in phase with the applied force (whatever the direction) at the rim of the disc, when the disc moves as a rigid body ($k_2a<1$).

(ii) When $k_2a>1$, if an inclined force is applied to the disc rim, the response at the centre of the disc will move in a different direction from the applied force. The response will however, be a vibration in a single direction provided a resonance is not excited.

(iii) If the excitation frequency $\alpha+\Omega$ rads/sec coincides with a resonance frequency, the centre of the disc will adopt an anticlockwise circling motion at α rads/sec. Likewise if the excitation frequency $\alpha-\Omega$ rads/sec coincides with a resonance frequency the centre of the disc will adopt a clockwise circling motion of α rads/sec.

REFERENCES

1. Love A.E.H. Mathematical Theory of Elasticity pp288 (Dover) New York.
2. Timoshenko S. and Goodier J.N. Theory of Elasticity (McGraw Hill).
3. A. Cemal Eringen. Response of an Elastic Disc to Impact and Moving Loads. Quart. Journal of Mechanics and Applied Mathematics Vol V111 Pt 4 (1955).
4. G. Ambati and J.J.W. Bell, J.C.K. Sharp. In plane vibrations of annular rings. J.S.V. (1976) 47(3), 415-432.
5. V.Srinvasan and V. Ramanarti. Dynamic Response of an Annular Disc to a Moving Concentrated, In-plane Edge Load. JSV (1980) 72(2) 251-262.
6. R.Holland. Numerical Studies of Elastic Disc contour modes lacking axial symmetry. JASA 1966, 40, 1051-1057.
7. E. Kreyszig. Advanced Engineering Mathematics, Chapter 3, John Wiley & Sons Inc. 1972.
8. M. Abramowitz and J.A. Segan. Handbook of Mathematical Functions p.369-371, Dover Publications.

APPENDIX A1: Formulation of the Problem

A1.1 The dynamic analyses of isotropic, homogeneous two dimensional solids is best performed in terms of 'dilatation' ε (or volume expansion) at a point and the 'rotation' ψ at a point. Expressed in terms of cartesian co-ordinates for the element below

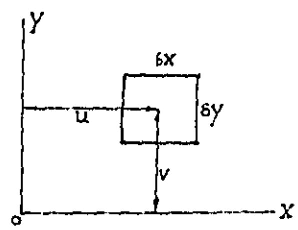

$$\varepsilon(x,y,t) \text{ (the total element strain)} = \frac{\partial u}{\partial x} + \frac{\partial v}{\partial y}$$

$$\psi(x,y,t) \text{ (the average element rotation)} = \tfrac{1}{2}\left(\frac{\partial v}{\partial x} - \frac{\partial u}{\partial y}\right)$$

Alternatively in plane polar coordinates, the displacements

$$\varepsilon(r,\theta,t) = \frac{1}{r}\left|\frac{\partial}{\partial r}(ru) + \frac{\partial v}{\partial \theta}\right|$$

$$\psi(r,\theta,t) = \frac{1}{2r}\left|\frac{\partial}{\partial r}(rv) - \frac{\partial u}{\partial \theta}\right| \qquad \text{(A1.1)}$$

$$u(r,\theta,t) \quad v(r,\theta,t)$$

where u and v are the displacements in the r and θ directions, as seen in the figure below

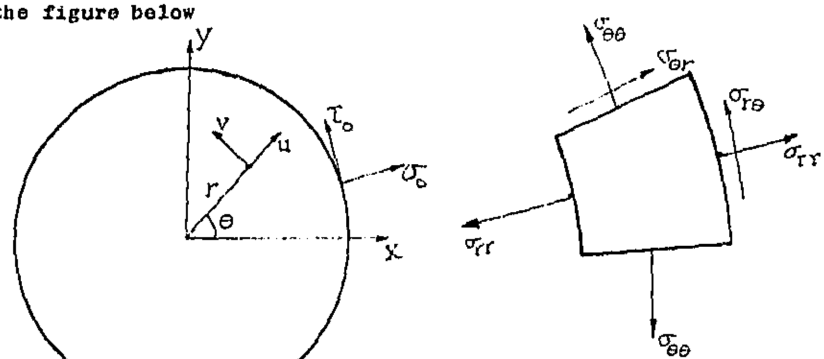

Figure A1.1

The Hookes Law relationship on a plane polar element is given |Ref 1 p288| as

$$\sigma_{rr} = \lambda\varepsilon + 2\mu\frac{\partial u}{\partial r}, \qquad \sigma_{r\theta} = \frac{\mu}{r}\frac{\partial u}{\partial \theta} + \mu r\frac{\partial}{\partial r}\left(\frac{v}{r}\right) \tag{A1.2}$$

$$\sigma_{\theta\theta} = \lambda\varepsilon + 2\,\frac{\mu}{r}.\left(\frac{\partial v}{\partial \theta} + u\right)$$

where λ and μ are defined in |1,p11,497| for a thick disc, as

$$\lambda = \frac{\nu E}{(1+\nu)(1-2\nu)}, \quad \mu = \frac{E}{2(1+\nu)}, \tag{A1.3}$$

μ is the material shear modulus; however for a thin disc

$$\lambda = \frac{\nu E}{(1-\nu^2)}, \quad \mu = \frac{E}{2(1+\nu)}$$

From the dynamic equilibrium of a plane polar element it can be shown |1 p288| that the equations of motion are

$$(\lambda+2\mu)\frac{\partial \varepsilon}{\partial r} - \frac{2\mu}{r}\frac{\partial \psi}{\partial \theta} = \rho\frac{\partial^2 u}{\partial t^2}$$

$$(\lambda+2\mu)\frac{1}{r}.\frac{\partial \varepsilon}{\partial \theta} + 2\mu\frac{\partial \psi}{\partial r} = \rho\frac{\partial^2 v}{\partial t^2} \tag{A1.4}$$

where ρ is the material density.

Eliminating u and v using equations A1.1 and A1.4 leads to the two uncoupled wave equations for dilatational and rotational motion.

$$\nabla^2\varepsilon = \frac{1}{C_1^2}\frac{\partial^2 \varepsilon}{\partial t^2} \qquad C_1^2 = (\lambda+2\mu)/\rho$$

$$\nabla^2\psi = \frac{1}{C_2^2}\frac{\partial^2 \psi}{\partial t^2} \qquad C_2^2 = \mu/\rho \tag{A1.5}$$

where C_1 and C_2 are the dilatational and rotational wavespeeds and ∇^2 is the Laplacian operator in plane polar coordinates i.e.

$$\nabla^2 = \frac{\partial^2}{\partial r^2} + \frac{1}{r}\frac{\partial}{\partial r} + \frac{1}{r^2}\frac{\partial^2}{\partial \theta^2}$$

The solution for the disc motion which conforms to the wave equations A15 must also satisfy the boundary conditions at the rim of the disc i.e.

$$\sigma_{rr}(a,\theta,t) = \sigma_o(\theta,t), \quad \sigma_{r\theta}(a,\theta,t) = \tau_o(\theta,t) \qquad \text{(A1.6)}$$

where σ_o and τ_o are the normal stress distributions and the shearing stress distributions applied to the rim in the direction indicated in Figure A1. It is assumed that no $\sigma_{\theta\theta}$ stress is applied.

A1.2 The Solution

If it is assumed that the time and space dependence of ψ and ε are separable functions, i.e. ψ and ε each take the form $A(r,\theta).B(t)$ then Fourier Transforms may be taken at both sides of equation A1.5. giving

$$(\nabla^2 + k_1^2)\,\bar{\varepsilon} = 0 \qquad k_1 = \omega/c_1$$

$$(\nabla^2 + k_2^2)\,\bar{\psi} = 0 \qquad k_2 = \omega/c_2 \qquad \text{(A1.7)}$$

where the $\bar{}$ denotes the Fourier Transform, defined as

$$\bar{\varepsilon}\,(\omega) = \int_{-\infty}^{\infty} \varepsilon(t)e^{-i\omega t}\,dt \qquad \text{(A1.8)}$$

k_1 and k_2 are the wave numbers associated with the dilatational waves and the rotational waves.

It is now assumed that $\bar{\varepsilon}$ and $\bar{\psi}$ are each the product of two separable functions, one of r dependence and one of θ dependence i.e.

$$\bar{\varepsilon} = \bar{W}(r).\bar{Q}(\theta) \qquad \text{(A1.9)}$$

Substitution of A1.9 into Equation A1.7 results in the governing equations for the θ and r dependence:

$$\frac{d^2Q}{d\theta^2} + n^2Q = 0 \qquad n=0,1,2,3\ldots \text{(A1.10)}$$

and

$$r^2\frac{d^2W}{dr^2} + r\frac{dW}{dr} + ((k_1r)^2-n^2)\,W = 0 \qquad \text{(A1.11)}$$

Equation A1.10 is a second order differential equation which has a solution of the form

$$\bar{Q}(\theta) = C\cos n\theta + D\sin n\theta \qquad \text{(A1.12)}$$

where C and D are constants. Equation A1.11 is Bessel's equation of order n which have solutions

$$\bar{W}_n(k_1r) = C_nJ_n(k_1r) + D_nY_n(k_1r) \qquad \text{(A1.13)}$$

where J_n and Y_n are Bessel functions of the first and second kind, C_n and D_n are constants. Y_n goes to infinity when $k_1r \to 0$ (at the centre of the disc) therefore $D_n=0$ for this problem.

The general solution for the dilatation and the rotation is found by substituting equation A1.13 and A1.12 into A1.9 and taking the sum of the n solutions i.e.

$$\bar{\varepsilon} = \sum_{n=0}^{\infty} (A_{1n}\sin n\theta + A_{2n}\cos n\theta)\,J_n(k_1r)$$

$$\text{(A1.14)}$$

$$\bar{\psi} = \sum_{n=0}^{\infty} (B_{1n}\cos n\theta - B_{2n}\sin n\theta)\,J_n(k_2r)$$

A_{1n}, A_{2n}, B_{1n}, B_{2n} are constants which are determined by the force distribution on the rim of the disc. Note that a cos nθ or sin nθ variation around the disc is associated with a J_n radial variation.

It can be seen from equations A1.14 that the dilatation at any point on the disc is entirely independent of the rotation. However the in plane displacements u,v, are a combination of dilatation and rotation effects and can be found |1| by substituting A1.14 into A1.1 (after taking Fourier Transforms of A1.1) and solving the resulting simultaneous partial differential equations to give:

$$\bar{u}(r) = \sum_{n=0}^{\infty} U_{1n}(r)\sin n\theta + U_{2n}(r)\cos n\theta$$

A1.15

$$\bar{v}(r) = \sum_{n=0}^{\infty} V_{1n}(r)\cos n\theta - V_{2n}(r)\sin n\theta$$

where

$$-r^{-1}\, U_{jn}(r) = A_{jn}\frac{1}{k_1 r}\cdot J_n'(k_1 r) + B_{jn}\cdot\frac{2n}{(k_2 r)^2}\cdot J_n(k_2 r)$$

$$-r^{-1} V_{jn}(r) = A_{jn}\cdot\frac{n}{(k_1 r)^2}\cdot J_n(k_1 r) + B_{jn}\cdot\frac{2}{(k_2 r)}\cdot J_n'(k_2 r)$$

$$j = 1,2.$$

The stresses at any point in the disc can be found by substituting equations A1.15 and A1.14 into A1.2 to obtain,

$$\bar{\sigma}_{rr}/(2\mu) = \sum_{n=0}^{\infty}\left[A_{1n}N_{1n}(k_1 r) + B_{1n}N_{2n}(k_2 r)\right]\sin n\theta +$$

$$+\left[A_{2n}N_{1n}(k_1 r) + B_{2n}N_{2n}(k_2 r)\right]\cos n\theta$$

$$\bar{\sigma}_{r\theta}/(2\mu) = \sum_{n=0}^{\infty}\left[A_{1n}S_{1n}(k_1 r) + B_{1n}S_{2n}(k_1 r)\right]\cos n\theta$$

$$-\left[A_{2n}S_{1n}(k_1 r) + B_{2n}S_{2n}(k_1 r)\right]\sin n\theta$$

$$\bar{\sigma}_{\theta\theta}/(2\mu) = \sum_{n=0}^{\infty} \left[A_{1n}\, T_{1n}(k_1 r) + B_{1n} T_{2n}(k_2 r)\right] \sin n\theta + \qquad \text{(A1.16) cont}$$

$$+ \left[A_{2n} T_{1n}(k_1 r) + B_{2n} T_{2n}(k_2 r)\right] \cos n\theta$$

where

$$N_{1n}(k_1 r) = (\lambda/2\mu)\, J_n(k_1 r) - J_n''(k_1 r)$$

$$N_{2n}(k_2 r) = \frac{2n}{(k_2 r)^2} . J_n(k_2 r) - \frac{2n}{(k_2 r)} . J_n'(k_2 r)$$

$$S_{1n}(k_1 r) = \frac{n}{(k_1 r)^2} . J_n(k_1 r) - \frac{n}{k_1 r} . J_n'(k_1 r)$$

$$S_{2n}(k_2 r) = \left(1 - \frac{2n^2}{(k_2 r)^2}\right) J_n(k_2 r) + \frac{2}{k_2 r} . J_n'(k_2 r) \qquad \text{(A1.17)}$$

$$T_{1n}(k_1 r) = \left(\frac{\lambda}{2\mu}\right) . J_n(k_1 r) + \frac{n^2}{(k_1 r)^2} . J_n(k_1 r) - \frac{1}{k_1 r} J_n'(k_1 r)$$

$$T_{2n}(k_2 r) = -N_{2n}(k_2 r)$$

The constants A_{1n}, A_{2n}, B_{1n}, and B_{2n} are all that are now required for a complete solution, and these are found by equating the Fourier Transform of the boundary conditions (Equation A1.6) to the equations A1.16 namely

$$\bar{\sigma}_o(\theta,\omega) = \bar{\sigma}_{rr}(a,\theta,\omega), \quad \bar{\tau}_o(\theta,\omega) = \bar{\sigma}_{r\theta}(a,\theta,\omega) \qquad \text{(A1.18)}$$

and multiplying both sides of equations A1.16 by cos $n\theta$ and sin $n\theta$ and integrating over a range $0 < \theta < 2\pi$. This procedure identifies the individual constants as

$$A_{1n} = [2\mu D_n]^{-1} . [S_{2n}(k_2a)\ \bar{\sigma}_{os} - N_{2n}(k_2a)\ \bar{\tau}_{oc}]$$

$$B_{1n} = [2\mu D_n]^{-1} .\ [-S_{1n}(k_1a)\ \bar{\sigma}_{os} + N_{1n}(k_1a)\ \bar{\tau}_{oc}]$$

$$A_{2n} = [2\mu D_n]^{-1} . [-S_{2n}(k_1a)\ \bar{\sigma}_{oc} + N_{2n}(k_2a)\ \bar{\tau}_{os}]$$

$$B_{2n} = [2\mu D_n]^{-1} . [-S_{1n}(k_1a)\ \bar{\sigma}_{oc} - N_{1n}(k_1a)\ \bar{\tau}_{os}] \qquad \text{(A1.19)}$$

$$n = 1,2,3.....$$

$$A_{jo} = \tfrac{1}{2}\ |A_{jn}|_{n=0} \qquad B_{jo} = \tfrac{1}{2}|B_{jn}|_{n=0} \qquad j = 1,2$$

$$D_n = N_{1n}\ (k_1a)\ S_{2n}(k_2a) - N_{2n}(k_2a)\ S_{1n}(k_1a)$$

where

$$\bar{\sigma}_{oc} = \frac{1}{\pi} \int_0^{2\pi} \bar{\sigma}_o(\theta,\omega)\ \cos n\theta\ d\theta$$

$$\bar{\sigma}_{os} = \frac{1}{\pi} \int_0^{2\pi} \bar{\sigma}_o(\theta,\omega)\ \sin n\theta\ d\theta \qquad \text{(A1.20)}$$

$\bar{\tau}_{oc}$ and $\bar{\tau}_{os}$ are similarly defined.

k_1/k_2 ν	.706 0	.666 .1	.612 .2	.55 .28	.503 .33	.403 .4	0 .5	Mode
	2.48	2.58	2.69	2.79	2.85	2.94	3.05	1.1
	5.01	5.31	5.78	6.318	6.54			1.1
	6.74	6.75	6.80	6.99	7.441	6.6	6.71	2.1
	9.60	9.87						2.1
	10.09	10.42	9.94	9.96	9.97	9.21	9.97	3.1
			11.28	12.56		10.03		
	13.15	13.15	13.17	13.20	13.13	13.14	13.17	4.1
	14.28	15.14	16.27		13.82			
	16.34	16.34	16.58	16.34	16.37	16.32	16.34	5.1
	18.57	19.49		18.36		17.29		
	19.52	19.93	19.50	19.52	19.49	19.51	19.51	6.1

TABLE 1: k_2a as a function of Poissons ratio for the (m,1) modes of dilatational and rotation of a thick disc (cylinder)

$$k_2 = 2\pi f \sqrt{\frac{2\rho(1+\nu)}{E}}$$

$$\frac{k_1}{k_2} = \sqrt{\frac{1-2\nu}{2-2\nu}}$$

$(\underline{m,1})$ = rotational mode

(m,1) = dilatational mode

ν	0.25	0.3	0.35	0.4	0.45	0,5
	1.652	1.617	1.578	1.5346	1.483	1,429
	3.536	3.5291	3,511	3.470	3.393	3.2764
	4.168	4.0474	3.933	3.837	3.771	3.738
	6.087	5.886	5.676	5.457	5.227	4,986
	6.9117	6.911	6,910	6.905	6.837	6.568
	8.0685	7.798	7.519	7.236	7.003	6.955
	9.9662	9.659	9.314	8.951	8,572	8,175
	10.1415	10.113	10.110	10.110	10.097	9.749
	11.948	11.544	11.126	10.692	10.2541	10.129

$$k_2 = 2\pi f \sqrt{\frac{2\ (1+\nu)}{E}}$$

$$\frac{k_1}{k_2} = \sqrt{\frac{1-\nu}{2}}$$

TABLE 2: (Holland |4|, k_1a as a function of Poissons ratio ν for the (m,1) modes of dilatation and rotation of a thin disc

TABLE 3: k_2a for the (m,0) rotational modes of vibration of a thin or thick disc

Mode	k_2a
1,0	5.136
2,0	8.418
3,0	11.621
4,0	14.795
5,0	17.96

$$k_2a = 2\pi f\sqrt{\frac{2\rho(1+\nu)}{E}}$$

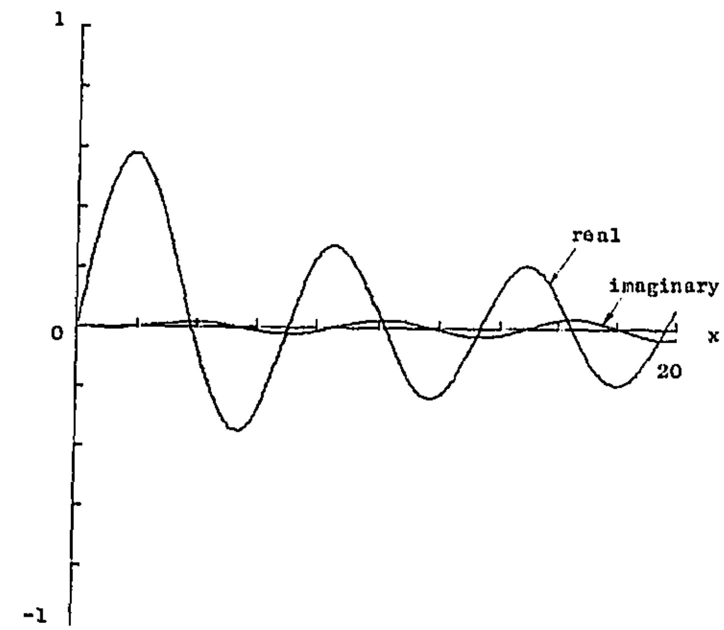

FIGURE 1: Complex Bessel function of the first kind of order 1, $J_1(x(1-.01i))$

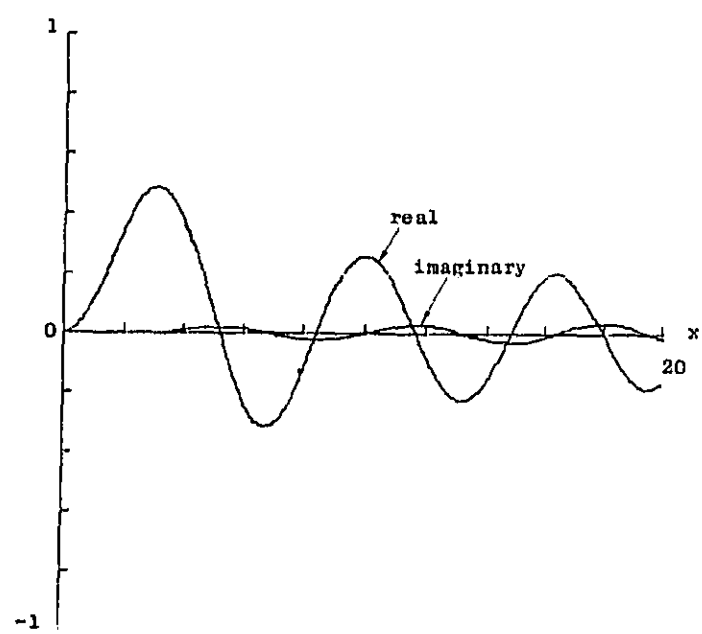

FIGURE 2: Complex Bessel Function of the first kind of order 2, $J_2(x(1-.01i))$

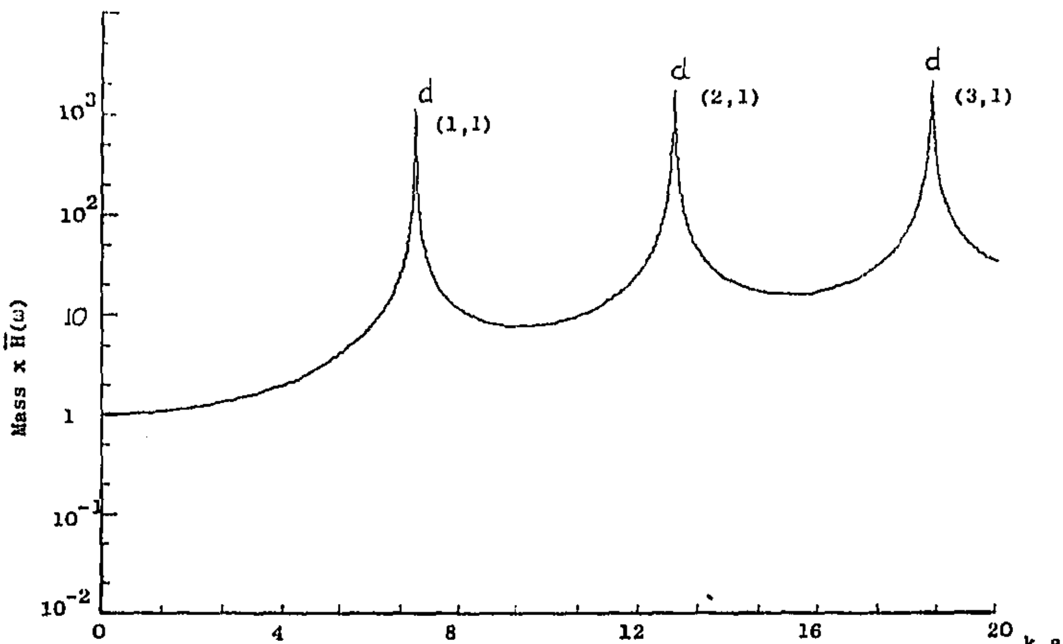

FIGURE 3: $|\overline{H}(\omega)|$ normalised to the disc mass $k_1/k_2 = .55$ for dilat ational waves alone

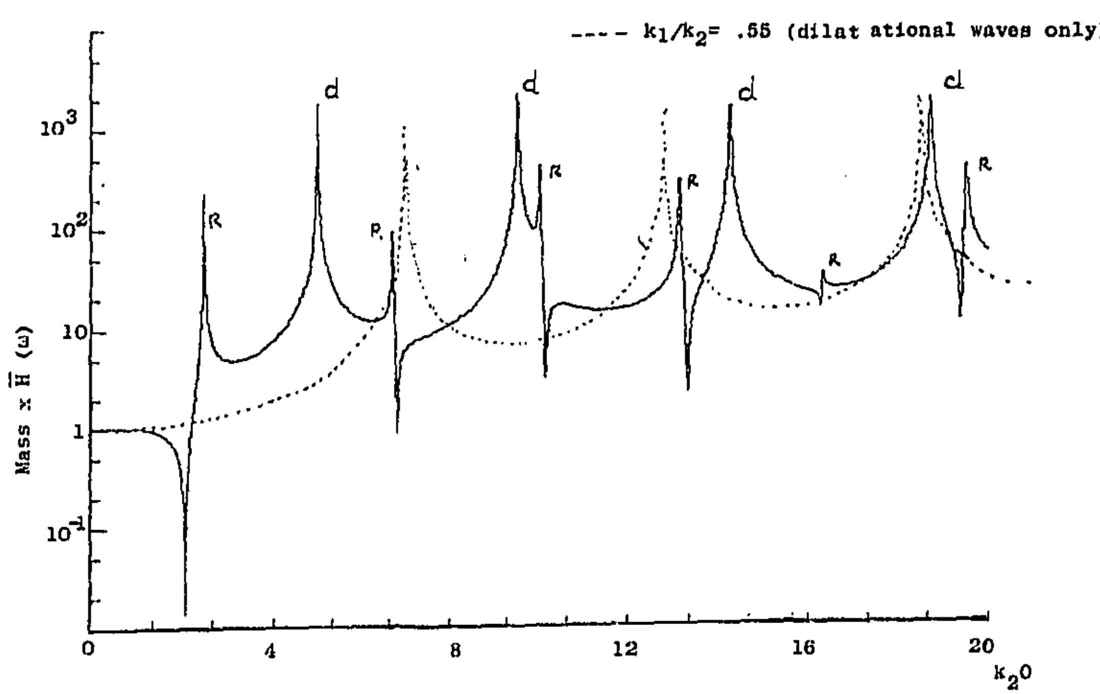

FIGURE 4: H(ω) x disc mass, Poissons Ratio = 0, $\frac{k_1}{k_2}$ = .706

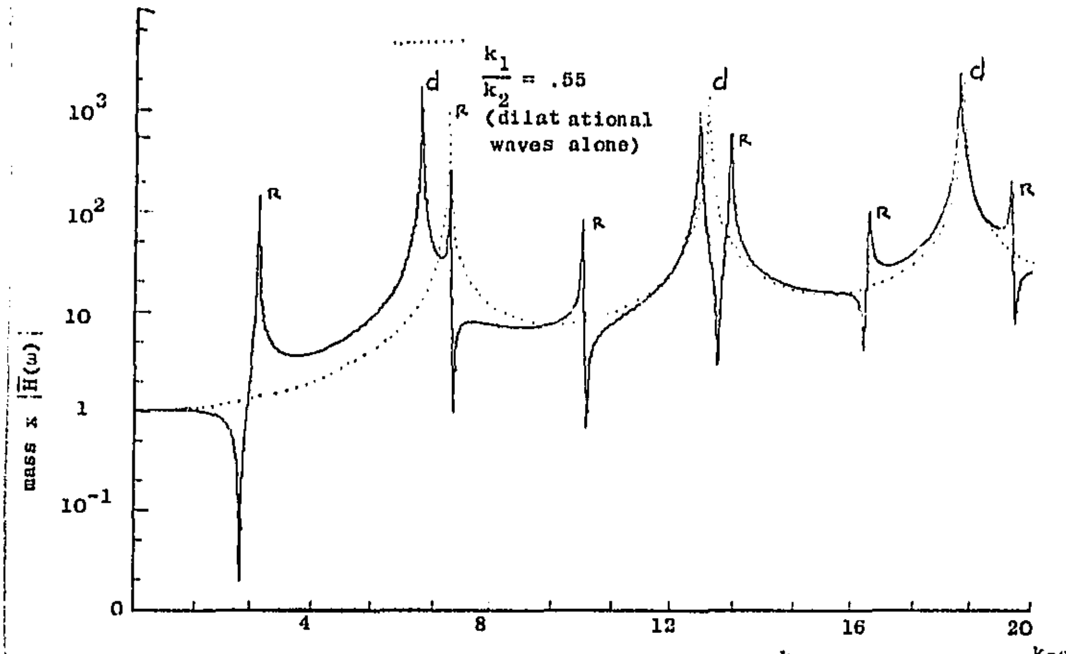

FIGURE 5: mass x $|\overline{H}(\omega)|$, Poissons ratio = .28, $\frac{k_1}{k_2} = .55$

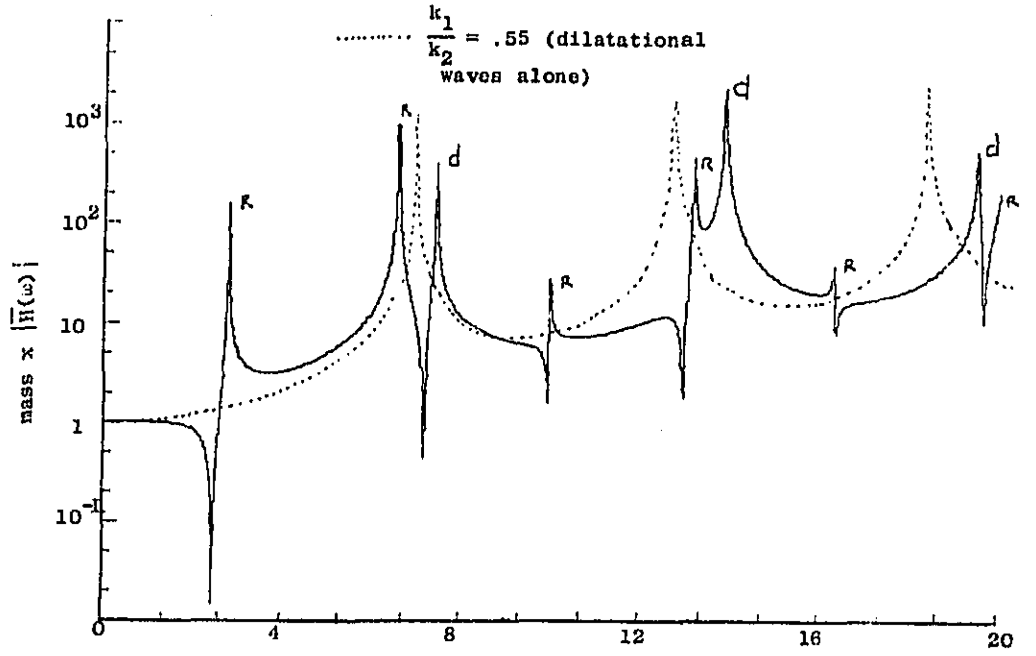

FIGURE 6: mass x $|\overline{H}(\omega)|$ Poissons Ratio = .33, $\frac{k_1}{k_2} = .503$

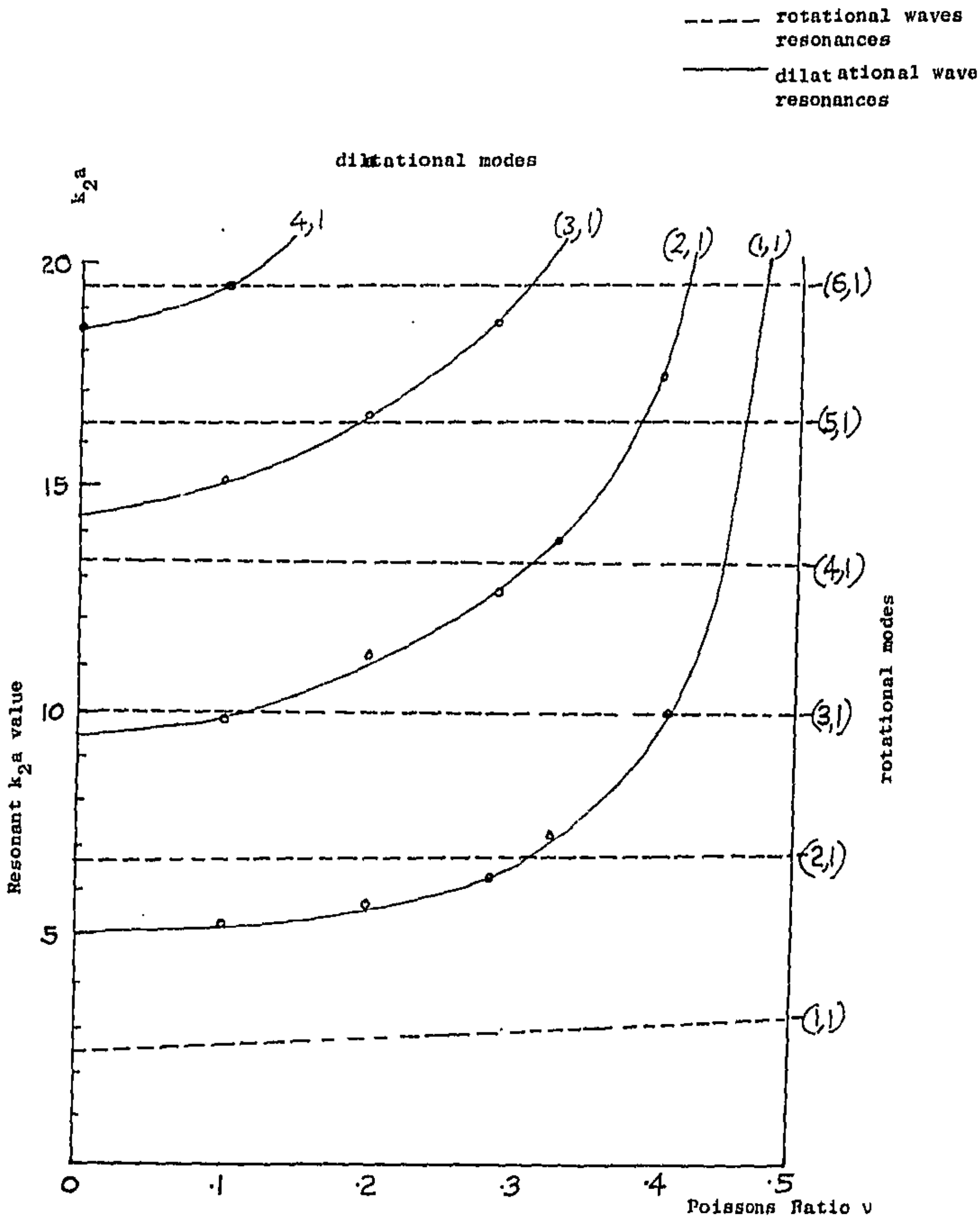

FIGURE 7: k_2a resonance values as a function of Poissons ratio, for a thick disc

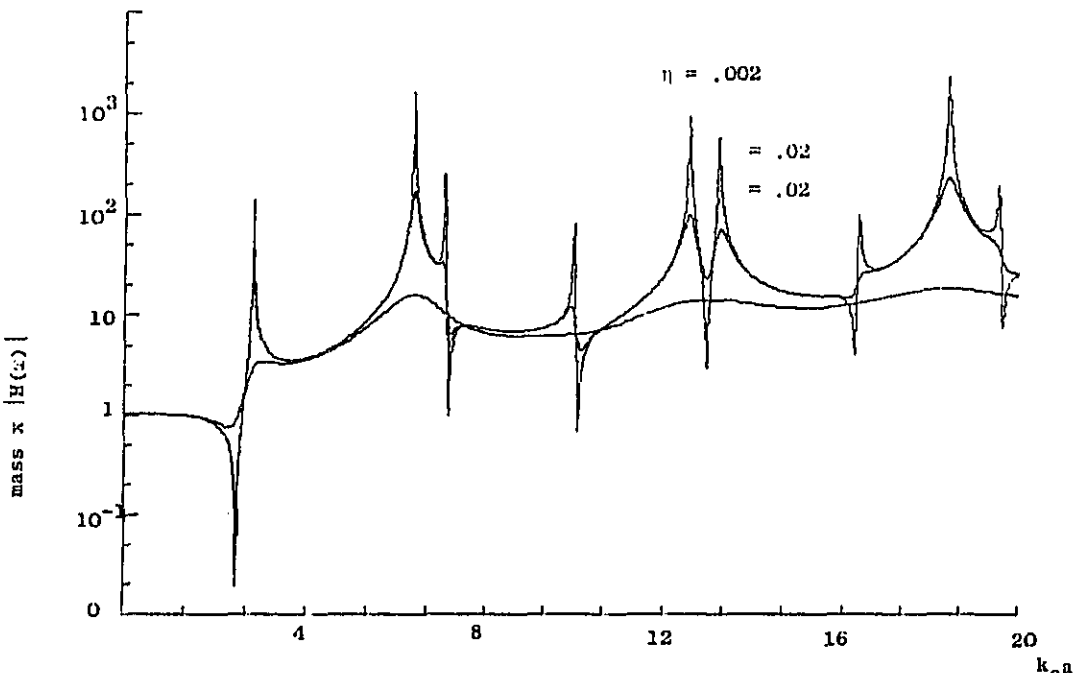

FIGURE 8: mass x $|\overline{H}(\omega)|$, k_1/k_2 = .55, η = .002, .02, .2

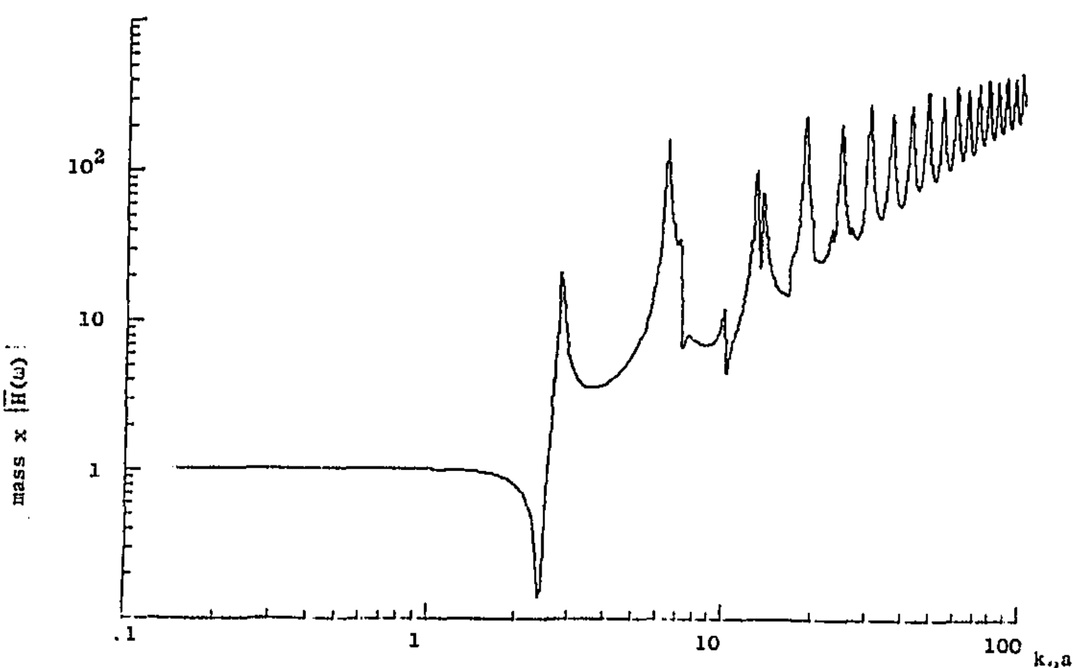

FIGURE 9: mass x $|\overline{H}(\overline{\omega})|$, $\frac{k_1}{k_2}$ = .55, η= .02

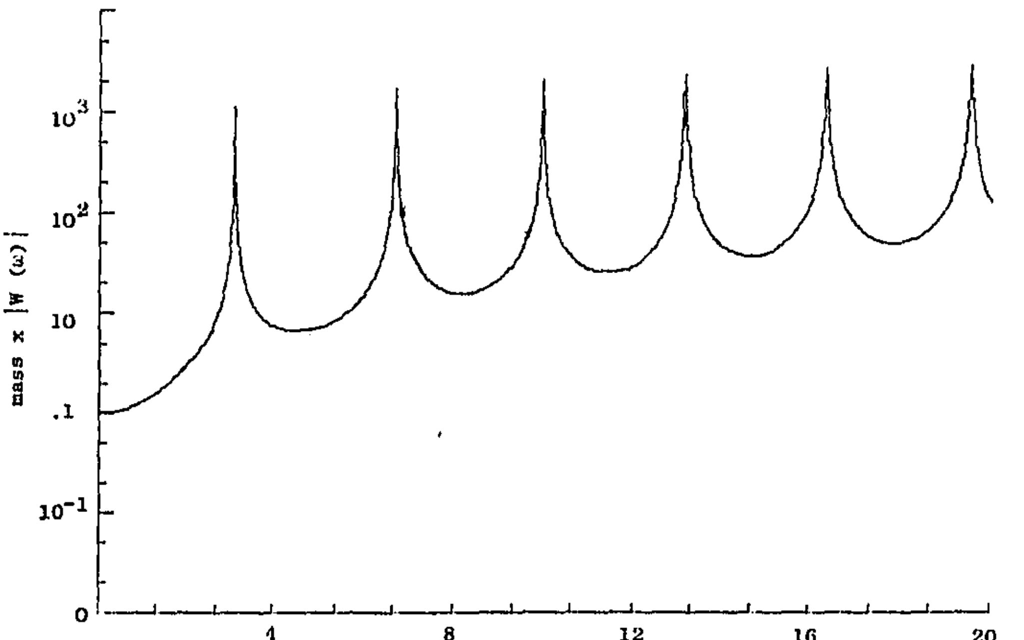

FIGURE 10: mass x $|W(\omega)|$ rotational wave alone $\frac{k_1}{k_2}$ = .01

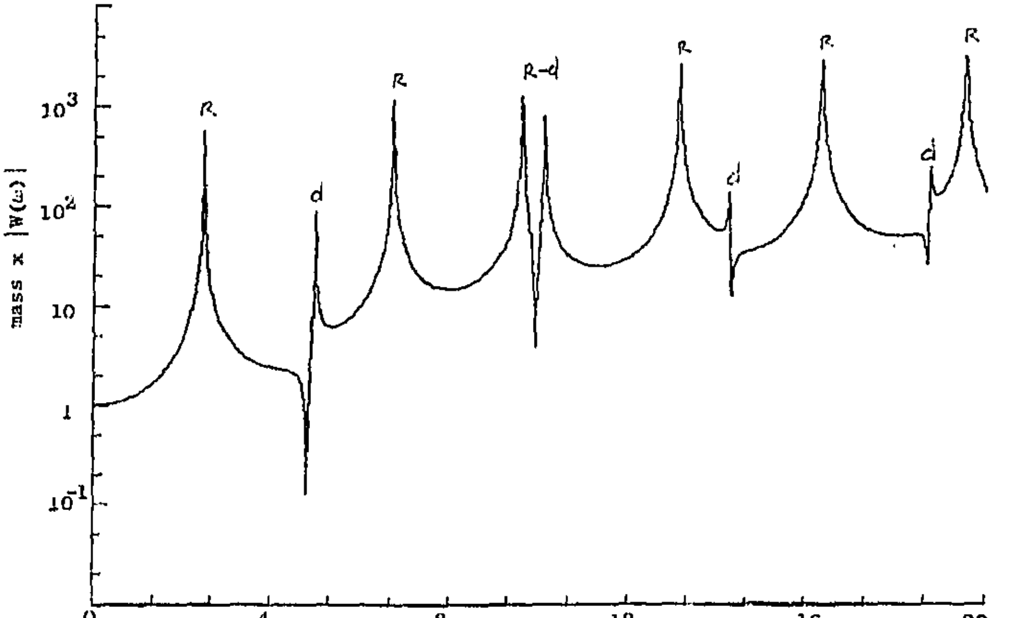

FIGURE 11 mass x $|W(\omega)|$, Poissons ratio = 0, $\frac{k_1}{k_2}$ = .706

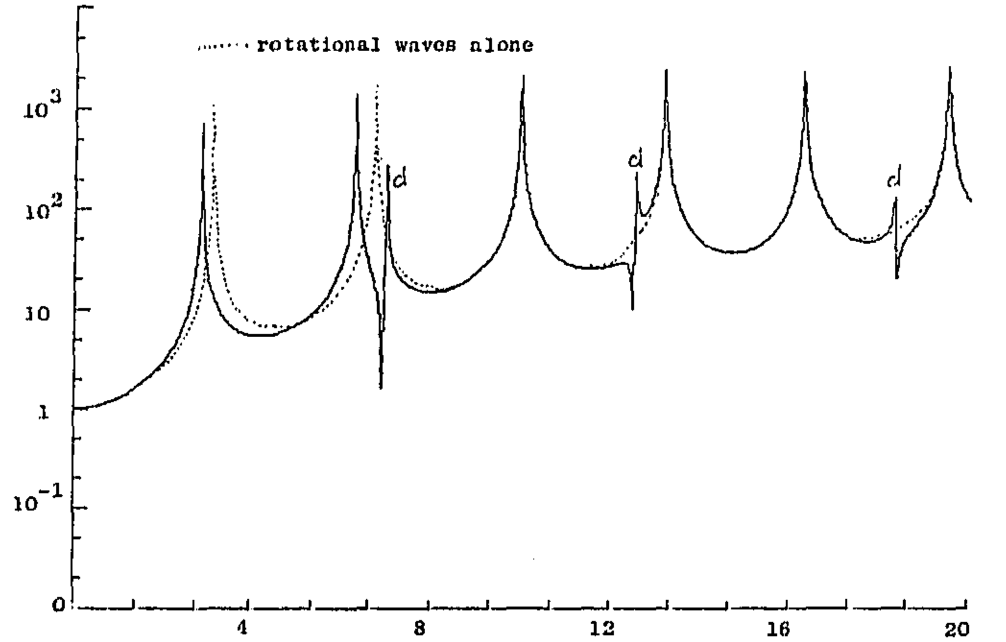

FIGURE 12: mass x $|W(\omega)|$, Poissons Ratio = .28, $\frac{k_1}{k_2}$ = .55

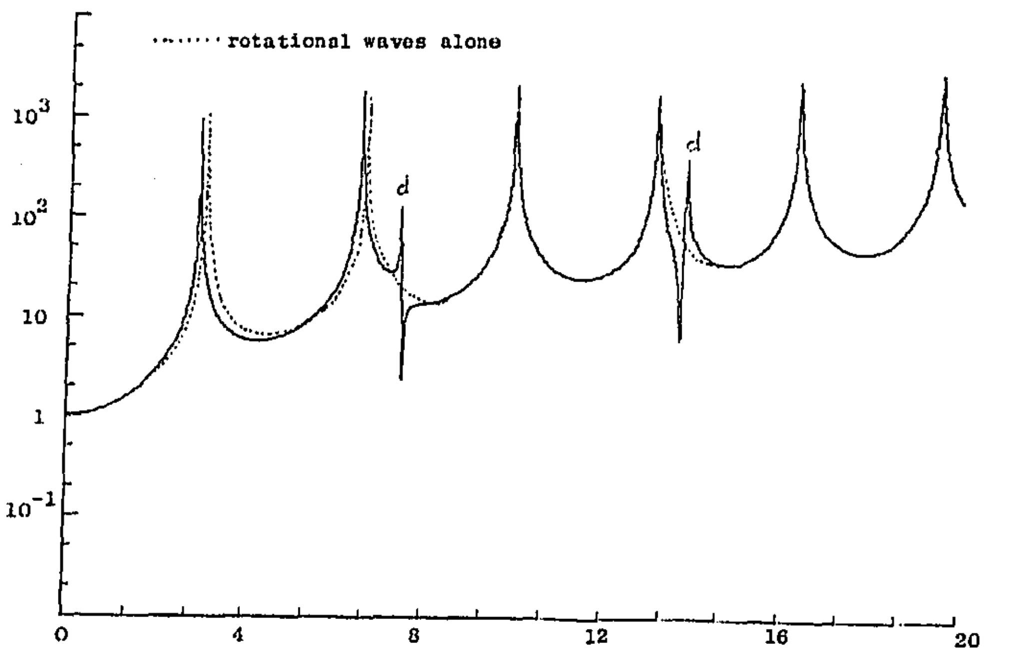

FIGURE 13: mass x $|\overline{W}(\omega)|$, Poissons Ratio, = .33, $\frac{k_1}{k_2}$ = .506

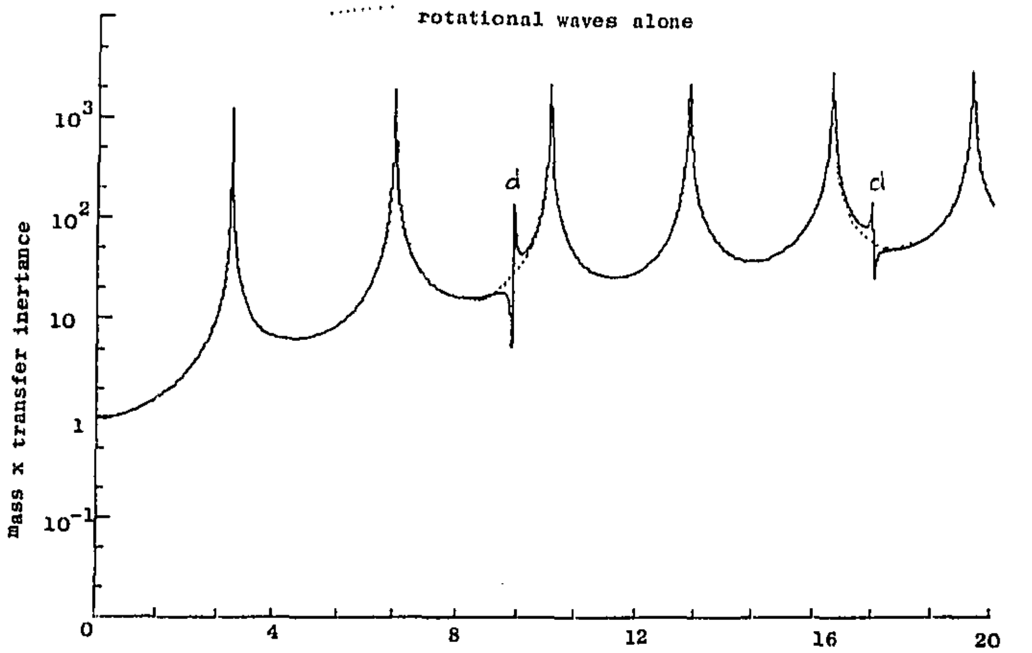

FIGURE 14: mass x $|\overline{W}(\omega)|$, Poissons Ratio = .4, k_1/k_2 = .403 k_2a

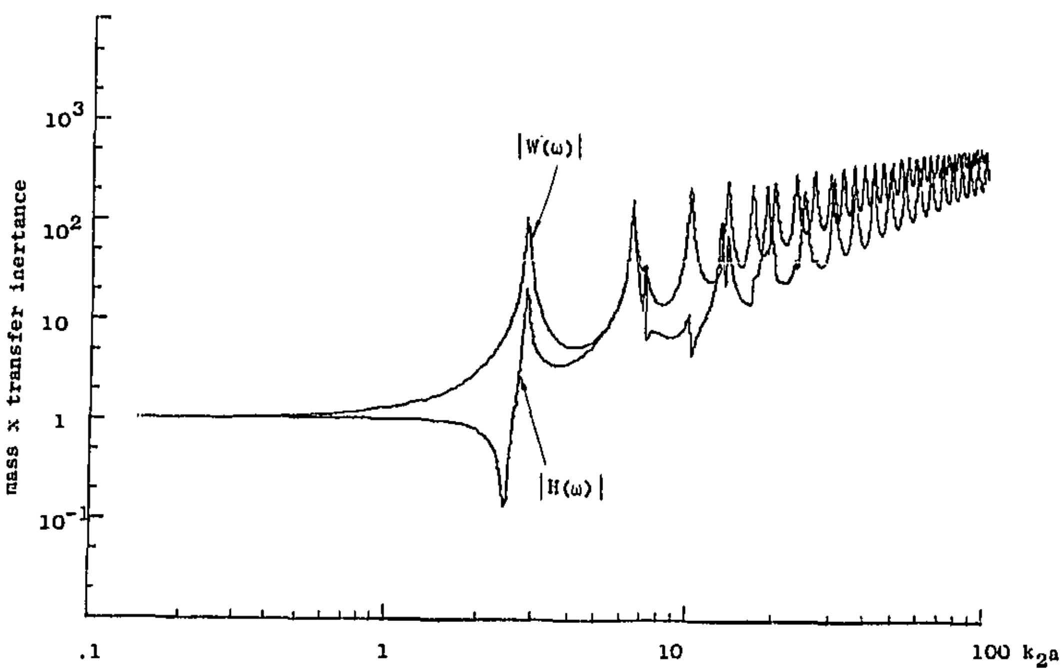

FIGURE 15: mass x $|W(\overline{\omega})|$, Poissons Ratio = .28, k_1/k_2 = .55 , η = .02
mass x $|H(\overline{\omega})|$

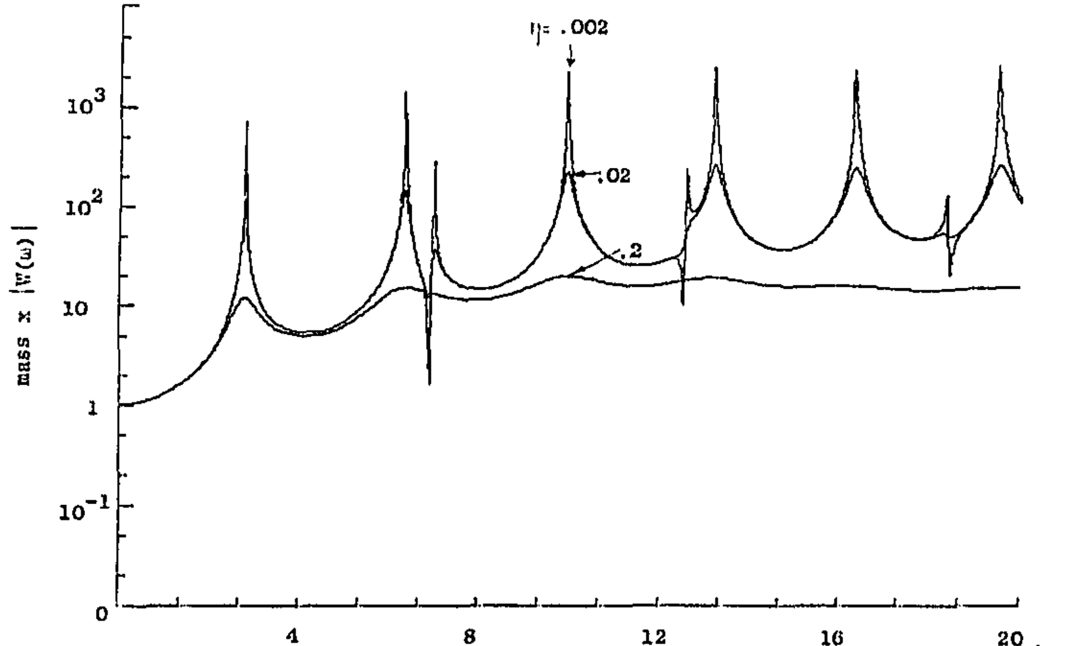

FIGURE 16: mass x $|W(\omega)|$ ν=.28 , $\frac{k_1}{k_2}$ .55
η = .002, .02, .2.

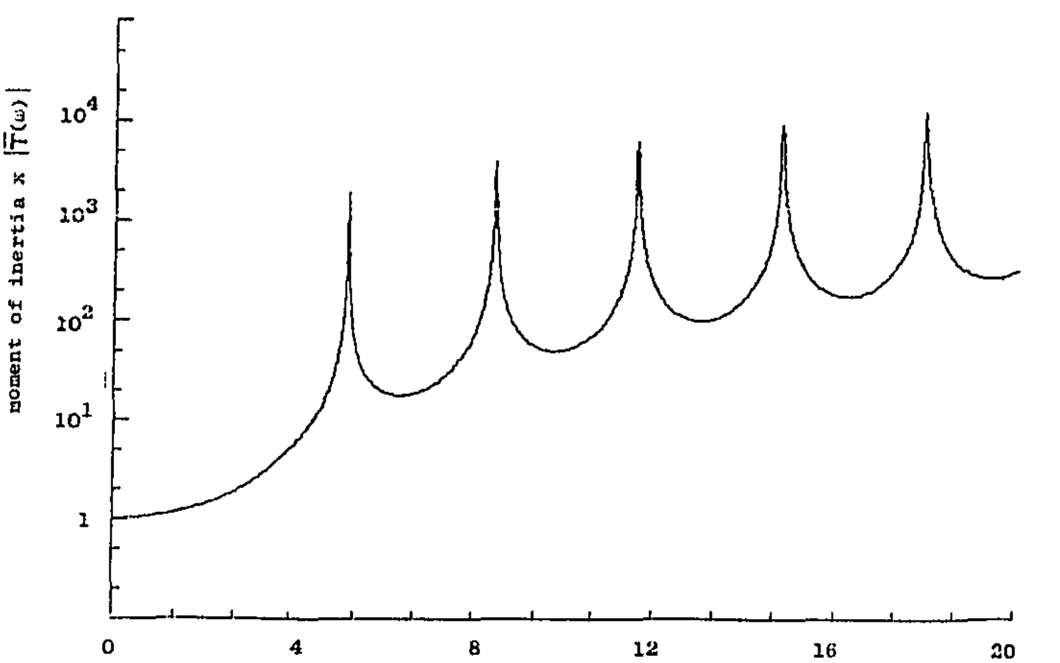

FIGURE 17: moment of inertia x $|\overline{T}(\omega)|$, η =.002

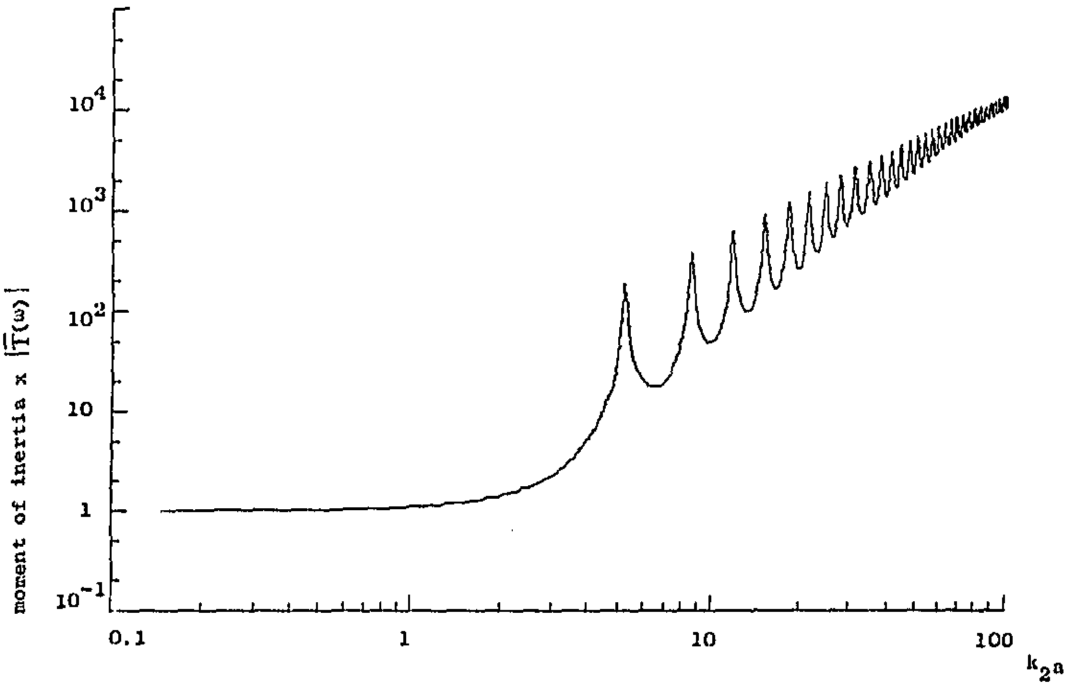

FIGURE 18: moment of inertia x $|\overline{T}(\omega)|$, $\eta = .02$